NASA CR-111849
N73-31018

NASA-CR-111849) DEVELOPMENT OF SYSTEM DESIGN INFORMATION FOR CARB N DIOXIDE USING AN AMINE TYPE SORBER Final Report, 18 Nov. 1969 - 12 Feb. (MSA Research Corp.) 91 p HC $6.75 CSCL 06K G3/05 14774

Unclas

Final Report

on

DEVELOPMENT OF SYSTEM DESIGN INFORMATION FOR CARBON DIOXIDE USING AN AMINE TYPE SORBER

(Contract No. NAS1-7263)

Prepared by

MSA RESEARCH CORPORATION
Evans City, Pennsylvania

for

National Aeronautics and Space Administration
Langley Research Center
Langley Station
Hampton, Virginia

June 15, 1971

DEVELOPMENT OF SYSTEM DESIGN INFORMATION FOR CARBON DIOXIDE USING AN AMINE TYPE SORBER

(Contract NAS1-7263)

by

R.L. Rankin
F. Roehlich
F. Vancheri

MSA RESEARCH CORPORATION
Evans City, Pennsylvania

June 15, 1971

Forward

This report has been prepared by MSA Research Corporation for the National Aeronautics and Space Administration's Langley Research Center under Contract No. NAS1-7263. The report covers work performed between 18 November 1969 and 12 February 1971.

Special appreciation is given to the contract technical monitor, Mr. R.B. Martin of Langley Research Center for his thoughtful guidance and cooperation.

Acknowledgement is expressed to MSA Research Corporation personnel.

Particularly to Mr. T.A. Ciarlariello who contributed significantly to much of the mathematical work included in the report and Mr. R. Bodesheim and J. King who aided in the experimental work.

TABLE OF CONTENTS

LIST OF FIGURES

LIST OF FIGURES (continued)

LIST OF TABLES

DEVELOPMENT OF SYSTEM DESIGN INFORMATION FOR CARBON DIOXIDE USING AN AMINE TYPE SORBER

by R.L. Rankin, F. Roehlich and F. Vancheri

SUMMARY

Experimental work was performed with pound quantities of IR-45 to determine the influence of particle size, process flowrate, bed L/D, sorber pretreatment, steam flowrate and CO_2 partial pressure on the absorption and regeneration processes.

The "as received", 16-60 mesh, IR-45 was segregated into three particle size ranges. These were >30 mesh, 30<>40 mesh and <40 mesh. Results obtained indicated that a 100% reduction of pressure drop with little difference in CO_2 sorption was offered by the >30 mesh particles compared with "as received" materials. Process flowrate and bed L/D tests showed that the sorption efficiency is reduced from 0.86 to 0.75, measured at bed half-life, as the residence time decreased from 1.5 to 0.7 seconds. Bed half life is defined as the condition when the bed effluent CO_2 concentration is 0.5 of the influent CO_2 concentration. No significant advantage was observed for residence times greater than 2 seconds.

Several pretreatment methods for reducing the trace contaminants off-gassed during cyclic absorption-regeneration of IR-45 were evaluated. Toluene was identified as the primary contaminant. Methanol extraction was found to be effective for reducing the toluene concentration from 10,000 to 200 μ gms/m^3. NASA-MSC was requested to evaluate IR-45 considering off-gassing, odor and flammability. IR-45 was rated "passing" for the three categories.

The effects of steam flowrate, particle size, bed L/D and IR-45 CO_2 concentration on regeneration rate, CO_2 recovery and concentrated CO_2 purity were determined. The steam flowrate was found to be most influential with no significant effect attributed to particle size or bed L/D. With steam flowrates in the 0.11 to 0.38 lb/hr range, 0.16 to 0.17 lb steam/lb dry IR-45 was required to regenerate an IR-45 bed. CO_2 recovery efficiencies greater than 95% were observed with a concentrated CO_2 purity of 98%.

The saturation capacity of IR-45 for CO_2 is related to CO_2 partial pressure in the 0.8 to 15 mm Hg range by:

$$\ln X^* = 1.2767 - 0.587/\sqrt{pCO_2}$$

Effects of multi-bed system designs were considered and the energy requirements and CO_2 capacity compared. A three-bed system offered a 24-32% reduction of energy per unit weight of CO_2 concentrated, compared to a one-bed design, but is penalized by system complexity.

The apparent heat capacity of IR-45 (dry) was determined as 0.29 Btu/lb-°F. Several materials including chamois and clays were surveyed as candidates for a dessicant type of zero-gravity condenser-steam generator. Vermiculite impregnated with LiCl appeared promising but migration of the LiCl is a problem in cyclic operation.

Experiments were performed with a 4-man size, single bed, system. The results of these tests were then reduced and a process model derived based upon the heat and mass balance associated with maintaining the IR-45 moisture content. Several model forms were considered with the best form including a correction for secondary condensation within the bed.

A CO_2 sorber comprised of a piperazine impregnated charcoal was studied attempting to alleviate some of the problems associated with IR-45. Moisture content, cycling, process flowrate and CO_2 partial pressure effects were considered. The charcoal was impregnated to 23 wt % and exposed to process operation. This CO_2 sorber exhibited a lesser dependence of CO_2 sorption on moisture content than IR-45, possessed a similar CO_2 capacity as IR-45 but tended to degrade with cyclic exposure.

Tests were also conducted with a sorber bed which was MOL prototype hardware to determine if this type bed, operating in a three-bed IR-45 system, would function to concentrate 0.375 lb CO_2/hr in the 90-day manned test performed for NASA by McDonnell Douglas Astronautics Company-Western Division. Also, in addition to testing, process design information was supplied Hamilton Standard Division of United Aircraft Corporation and close liason maintained in the system design. A recommendation that the three sorber beds with 7.0 lb of IR-45 in each bed could concentrate 0.375 lb CO_2/hr at 98% purity was forwarded to Hamilton Standard.

INTRODUCTION

This report describes experimental and analytical activities performed for the National Aeronautics and Space Administration - Langley Research Center during the period November 1969 through February 1971 on the Development of System Design Information for Carbon Dioxide Using an Amine Type Sorber.

Amberlite IR-45, an aminated Styrene divinylbenzene matrix, was investigated to determine the influence of the design parameters of sorber particle size, process flowrate, CO_2 partial pressure, total pressure and 1, 2 and 3 bed designs.

Task II entailed experimental and analytical effort to enable relating mathematically the CO_2 capacity and energy requirements of a 4-man size system to important operational parameters.

In Task III, a system was to be designed and fabricated using the information obtained in Tasks I and II. This task was modified, however, by NASA in order to substitute Task V.

Task IV activities included some fundamental studies with a CO_2 sorber which could offer advantages over the polymeric IR-45. CO_2 capacity, energy requirements and process operation were considered.

Task V was substituted for Task III in support of the polymeric type CO_2 concentration system used in the 90-day manned test performed by McDonnell Douglas Astronautics Company - Western Division for NASA. Activities of Task V included experimental work, analysis and supply of process information to Hamilton Standard Division of United Aircraft Corporation which fabricated the 90-day test system.

EXPERIMENTAL FACILITY

Test System

Task I experiments were performed with a test system which enabled control of the process flow temperature, humidity, CO_2 concentration and flow rate. Figure 1 illustrates this system. Plant air, used as the CO_2 carrier, was directed through a mechanical filter (400 mesh screen) and a silica gel-baralyme bed (1) to remove particulate, moisture and residual CO_2 before entering the test system. The filtered air entered the test system through one of two flow meters (2) (Brooks Rotameter, Model C-1307-08-G-G1-A) or Brooks Rotameter, Model 5-65-A) depending upon the desired flow rate range (272, 50 SCFH) and was then directed through a shell and tube heat exchanger (3) to achieve the desired sensible temperature. Humidification was achieved by flowing part of the thermally conditioned process air through an isothermal water column (4) and mixing with the bypassed flow downstream of the humidifier. CO_2 was injected into the process stream at the point of air mixing through a flow meter (5) (Brooks Rotameter, Model B07-08-5261-A).

Immediately upstream of the sorber bed (7) the CO_2 concentration and dewpoint of the process air were monitored with infrared analyzers (6) (MSA LIRA, Model 300) which have 50 and 100 ppm sensitivities for CO_2 and water, respectively. The CO_2 LIRA was calibrated with a 0.46 ± .005% mixture of CO_2 in nitrogen while the water LIRA was calibrated with a 39.0 ± .05% mixture of ethylene in nitrogen which corresponds to a dewpoint of 78.8°F. This calibration procedure for the water LIRA was permitted because ethylene has an absorption characteristic practically identical to water. The outlet of the LIRA's was returned to the process stream before entering the sorber bed to retain the system mass balance. Downstream of the sorber bed the effluent CO_2 concentration and dewpoint were monitored with LIRAs (8) similarly to the input.

Process air sensible and dewpoint temperatures in the range of 45-100°F were controlled to ± 2°F. All temperatures including sorber were monitored with the thermisters (9) (Fenwal Ka3265) calibrated to the boiling and ice point temperatures of water at atmospheric pressure.

Sorber Regeneration

Sorber regeneration was performed by heating the sorber with steam supplied from a 500 ml flask heated by a laboratory heating mantle (13). The regeneration apparatus is included in

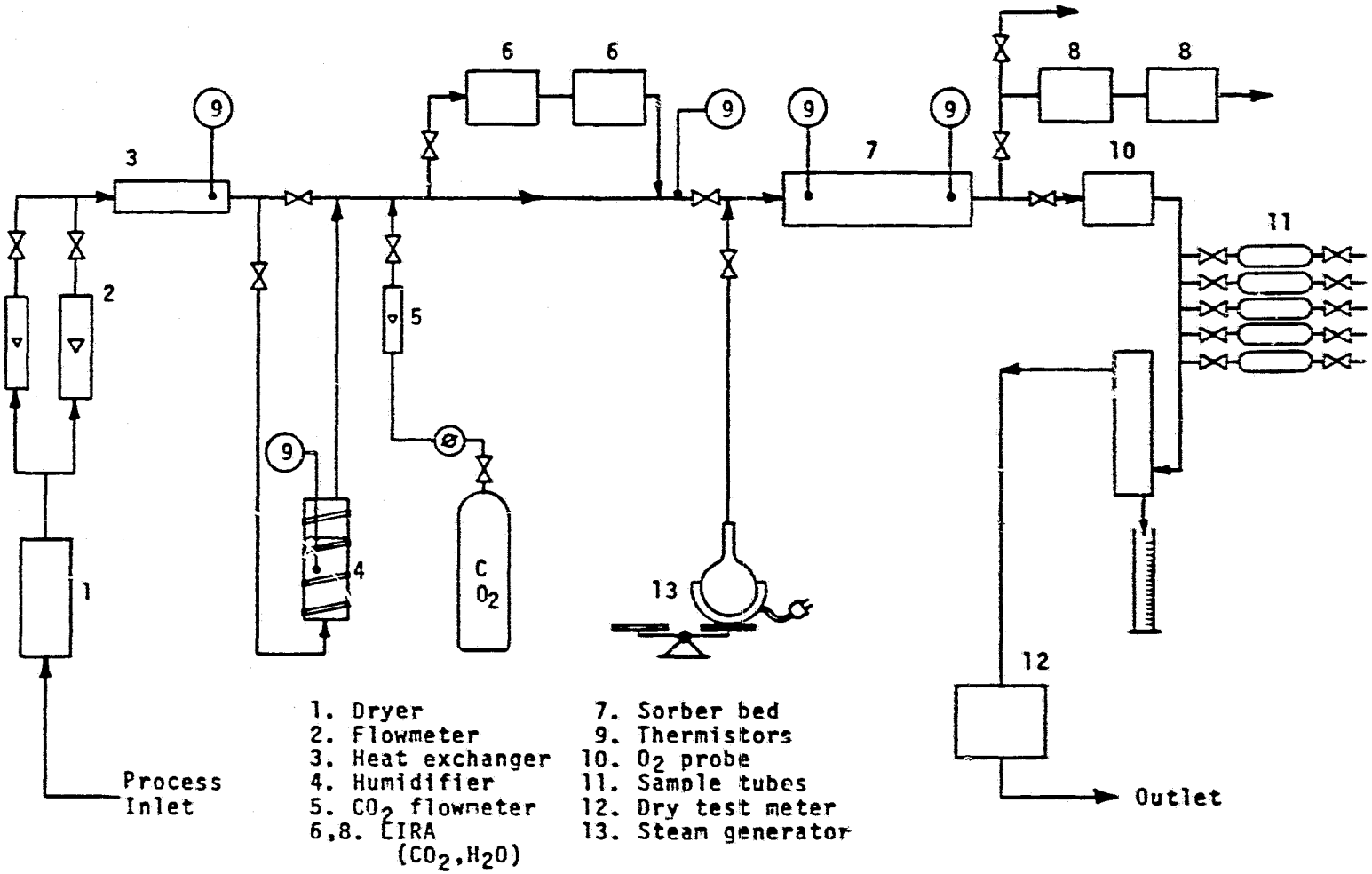

FIGURE 1 TASK I TEST SYSTEM

Figure 1. Steam delivery rates of 0.1-0.4 lb/hr were achieved by regulating the electrical power to the mantle. Observation of the flask weight difference with time determined the delivery rate and the thermal requirement for regeneration of the sorber was indicated by the total weight difference.

During the sorber regeneration, the air-CO_2 separation was determined by monitoring the decrease of oxygen concentration of the displaced gas mixture with a polarographic analyzer (10) (Beckman, Model 778). The actual composition of the displaced gas was determined by extracting 100 ml samples of the gas mixture for mass spectrometer analysis. The samples were extracted by directing the displaced gas mixture through glass tubes (11) immediately downstream of the oxygen monitor. Five sample tubes were fixed in a parallel bypass arrangement which permitted sampling in 15 second intervals. The displaced gas mixture flow rate and total flow were measured with a dry test meter (12) (NAR 150 CFH) located downstream of the sampling manifold.

Sorber Beds

Four beds for sorber containment were constructed of which three were glass and the fourth polyethylene base plastic. The glass beds were fabricated of 81 mm tubing closed at the ends with dished heads as illustrated by Figure 2. The dished head on the bed input end was flanged, "O" ring sealed and held to the tubing with a Marmon type clamp thereby permitting loading the beds. The dished head on the bed output end was minimized to reduce effluent gas mixing during the sorber regeneration. The beds provided length to diameter ratios of 1, 2 and 4/1.

Two temperature monitor penetrations were made through the bed side wall and thermistors sealed into the bed with a silicone sealant (GE RTV 615). Pressure taps in the bed wall and output dished head were provided for determining the sorber pressure drop which was read out with a manometer. Also part of the sorber beds was a device which indicated the sorber moisture content by measuring the electrical resistance of the sorber. This device was constructed of two platinum plates, 1.4 cm square, separated 1 cm; the sorber resistance was measured with an electrometer (Kiethley, Model 620) and compared to resistance values determined for sorber samples of known moisture content. Figure 3 presents the IR-45 resistance as related to moisture content. The sorber was held in the proper configuration in the beds by two "Nevaclog" separators cut to fit the glass tubing. "Nevaclog" is constructed of two perforated stainless steel sheets rotated such that the perforations are not colinear and spot welded. The "Nevaclog" possesses structural integrity not available with screens, does

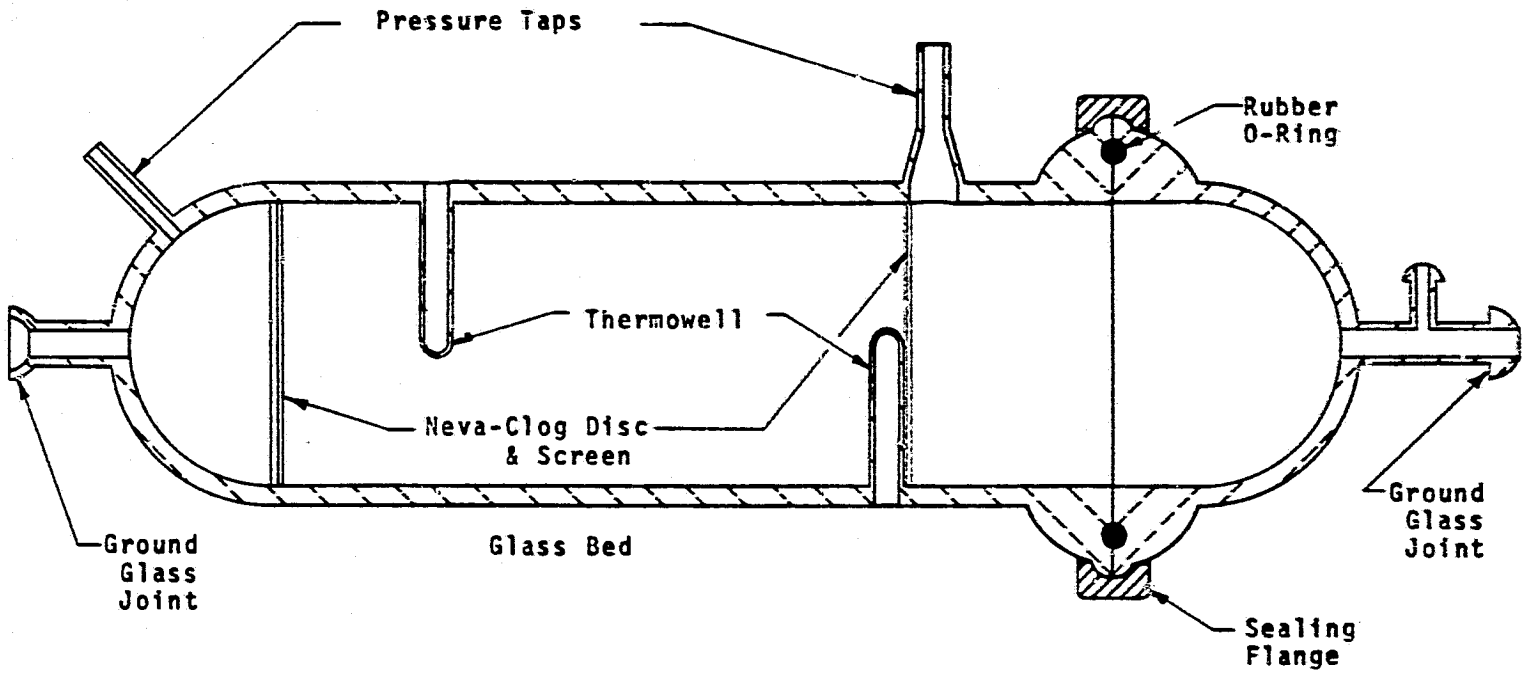

FIGURE 2 UNIT SORBER BED

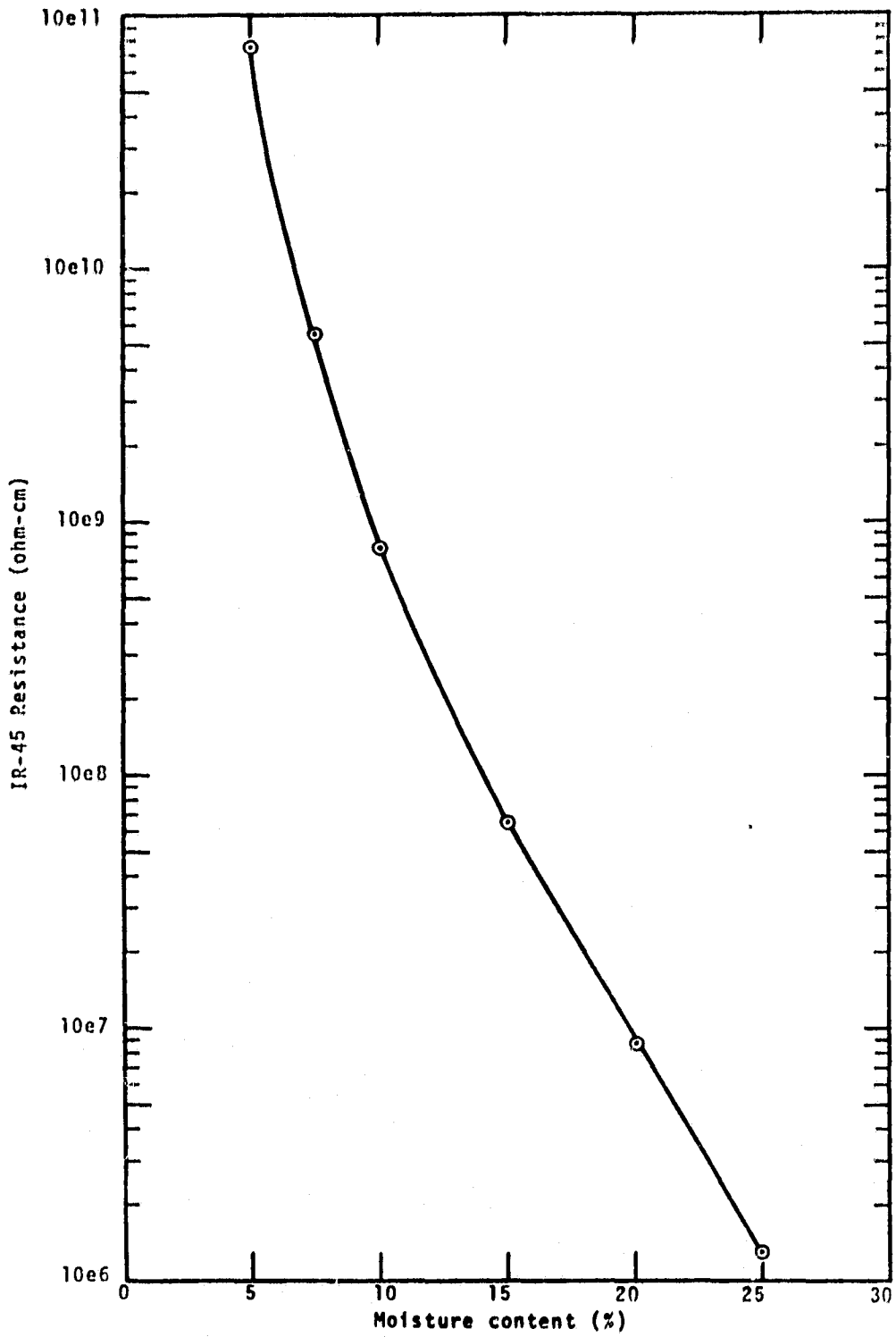

FIGURE 3 IR-45 MOISTURE CONTENT AND ELECTRICAL RESISTANCE

not "wick" water but permits flow velocities in excess of 100 fpm with less than 0.5 inches water pressure drop. One separator was sealed into the output end of the glass tubing while the other was held in place by a spring load. The beds were thermally insulated with laminations of 0.005 inch aluminum foil and Johns-Manville micro-quartz felt to a 0.75 inch thickness.

The fourth bed was 3 inch ID and was sectioned into 16 cells each 0.75 inches long. The cells were separated with 80 mesh stainless steel screen and the sorber was loaded into the cells through 0.375 inch tubes located radially on the perimeter. These loading tubes were closed with spring retained stoppers to prevent leakage through the tubes. Figure 4 illustrates the sectioned bed which was used to determine the CO_2 concentration gradient in the sorber bed for different bed effluent concentrations.

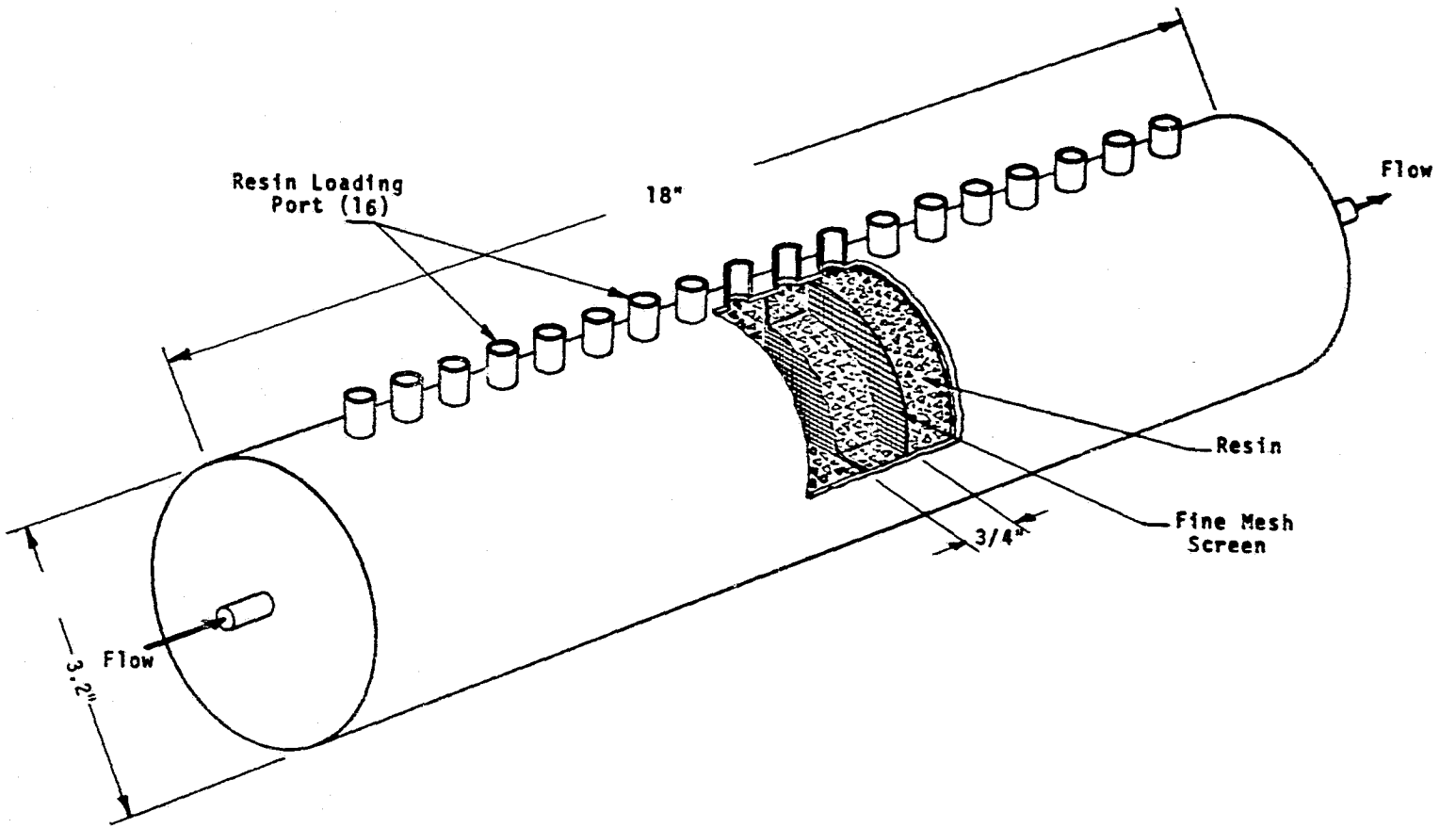

FIGURE 4 SECTIONED BED

TASK I PARAMETRIC STUDIES

Task 1.1 Sorber Particle Size Optimization

Minimizing the sorber bed pressure drop offers the advantage of reducing the power required to move a quantity of fluid, namely air or water, through the bed. Complementarily, system fixed weight may be reduced by sufficient pressure drop reduction. Ergin[1] has shown the pressure drop per unit depth of dry packed beds to be related to the packing surface A_p.

$$\frac{\Delta P}{Z} = \left[\frac{150(1-\varepsilon)}{Re} + 1.75\right](1-\varepsilon)G'^2/g'_c\varepsilon^3 d_p \zeta_G$$

where
- ΔP = Pressure drop (lb/ft^2)
- Z = Height of packing (ft)
- ε = Void fractions in a packed bed
- Re = Reynolds number for a particle, based on superficial gas velocity
- G' = Superficial mass velocity of gas based on empty bed cross section ($lb/hr\text{-}ft^2$)
- d_p = Diameter of a sphere whose surface volume ratio is the same as that of a packing particle (ft)
- ζ_g = Gas density (lb/ft^3)

and $d_p = 6(1-\varepsilon)/Ap$

Leva[2] approximates the pressure drop per unit depth of wet packed beds in terms of the shape factors, n, and m.

$$\frac{\Delta P}{Z} = m(10^{-\theta})(10^{nL'}/\zeta L)G'^2/\zeta G$$

where
- ΔP = Pressure drop (lb/ft^2)
- Z = Height of packing (ft)
- L' = Superficial mass velocity of liquid, based on empty bed cross section ($lb/hr\text{-}ft^2$)
- G' = Superficial mass velocity of gas, based on empty bed cross section ($lb/hr\text{-}ft^2$)
- ζL = liquid density (lb/ft^3)
- ζg = gas density (lb/ft^3)

Both relationships indicate a dependence of the bed pressure drop on a form of bed particle geometry. Some experiments performed under Contract NAS1-5277 suggested that the sorber bed pressure drop could be reduced by using particle sizes greater than 40 standard mesh with essentially equivalent dynamic CO_2 capacity as the "as received" particle distribution. The "as received" sorber

particle size distribution scaled by weight fraction is presented by Table 1.

TABLE 1 - MESH SIZE OF AS-RECEIVED IR-45

Mesh Size (U.S. Std. Sieve)	% Total Weight
+20	19.3
-20+30	46.7
-30+40	23.4
-40 (Fines)	10.6

For the present studies, the "as received" sorber was segregated into three particle mesh size ranges: >30 (coarse), 30<>40 (intermediate) and <40 (fines). Each size range was evaluated for CO_2 removal efficiency, capacity, bed pressure drop and regenerated CO_2 purity with testing in the unit beds having length to diameter ratios of 2 and 4 described by Figure 2 and the sectioned bed of Figure 4 and test system of Figure 1. These tests were performed with an air flow rate of 0.5 CFM, a sensible temperature of 70 ± 2°F, dew point 50 ± 2°F, input CO_2 partial pressure 3.7 mm Hg, sorber moisture content 5-7 wt % and 740 mm Hg total pressure. Initially, the process test conditions included a 15 wt% sorber moisture content. During the absorption tests however, the moisture content was decreased by evaporation to the air indicating non-equilibrium between the sorber and air humidity. Although a dynamic CO_2 capacity of 2.7 wt% was achieved with the 16-60 mesh particle size, constancy of conditions was denied by the transient heat and mass transfer affected by the evaporation. Subsequently, this problem was relieved by operating the sorber with 5-7 wt % moisture which was determined, under Contract NAS1-5277, to be in equilibrium with 70°F sensible, 50°F dew point air. Also, the lesser moisture content condition had the advantage of amplifying particle size effects. A steam flow rate of 0.31-0.35 lb/hr was used for both unit bed and sectioned bed sorber regeneration.

A comparison criteria (γ) for the CO_2 absorption results of the particle size effect tests was defined as the ratio of the theoretical velocity power required per pound of CO_2 absorbed.

$$\gamma = \dot{V}\Delta P/mCO_2$$

where $\dot{V}$ = volume flow rate

ΔP = pressure drop through sorber bed

mCO_2 = mass of CO_2 absorbed

This criteria permitted comparison of the sorber pressure drop and dynamic CO_2 capacity for each particle size range.

Each test was performed by establishing the desired conditions then placing the sorber bed in the process stream. Air temperatures and humidity, bed temperature, moisture content and pressure drop and bed input and output CO_2 concentrations were monitored until the bed output CO_2 concentration reached 0.5 of the input. The sorber bed was removed from the process stream and regenerated. During regeneration the steam generator weight, bed temperature, evolved gas flow rate, condensate quantity and oxygen content were monitored. When the evolved gas flow rate decreased to zero the regeneration was concluded and the sorber removed from the bed. A second bed of different length was placed in the process stream and the test sequence repeated.

Results.-A total of 23 distinct tests were performed to determine the optimal particle size range for the CO_2 removal and concentration system evaluation.

The >30 mesh particle range exhibited a definite advantage for CO_2 removal with a minimal power requirement. A velocity power to CO_2 mass ratio of 13 watts per pound CO_2 was determined for the >30 mesh size while the power to mass ratio for the <40 and 16<>40 mesh sizes were 60 and 26 watts per pound CO_2, respectively. The increase of the ratio reflects the increase of bed pressure drop from 3.5 to 13.3 in. H_2O/ft with decreasing particle size. The dynamic CO_2 capacity of each particle size bed was 1.1 ± .05 wt % at the bed half-life.

Table 2 presents the results for the three sorber particle sizes.

TABLE 2 - ABSORPTION CHARACTERISTICS OF IR-45 PARTICLE SIZES

Particle Size Mesh	L/D	Half-life Capacity (wt %)	Pressure Drop (in. H_2O)	watts γ(lb CO_2)
-40	4	1.15	13.5	62.4
-40	2	0.86	6.6	59.3
+30	4	1.05	3.5	13.2
+30	2	0.72	1.8	13.2
16<>60	4	1.11	5	28.6
16<>60	2	0.89	3.1	23.6

These data show that the <40 mesh particles provide a possible 10% advantage in capacity compared to the >30 size particles in the L/D = 4 beds. This advantage increases to 19.5% for the L/D = 2 beds. The velocity power expended to achieve the capacity advantage of the <40 mesh size, however, is greater by a factor of 4.6 than the power required by the >30 mesh size. The 16<>60 size exhibited an equivalent capacity to the <40 mesh size but required twice the power of the >30 mesh size. Figure 5 presents the results of the unit bed tests for the three particle sizes as breakthrough curves. These curves represent the time history of the 2 and 4 length to diameter ratio beds. Also described is a curve performed with a bed of unit L/D and <40 mesh particle. Figure 6 represents the same test data but illustrates the sorber CO_2 concentration related to the bed effluent CO_2 concentration.

Six tests were performed on the different particle sizes with the 16 unit sectioned bed to enable determining the CO_2 concentration distribution within the sorber bed. These tests were conducted similarly to the unit bed tests but were terminated when the bed output CO_2 concentration was initially detectable (>50 ppm). Each of the sections were regenerated and the evolved CO_2 quantity measured by displacement of the CO_2 saturated water. Figure 7 presents these results which show three different concentration sections of the bed. About three inches of the bed measured from the input attained a 0.9% CO_2 concentration approaching the saturation capacity of the sorber at the 5-7% moisture content. The succeeding five inches of bed contains the primary absorption wave or concentration gradient which traverses the bed during the total bed life and the remaining four inches of the bed shows nearly a constant CO_2 concentration of 0.18% for the <40 and 16<>60 mesh particles.

The >30 mesh particles exhibited a less distinct absorption wave than the other two particle sizes. However, the quantities of sorber per section of bed were sufficiently small (45 grams) that all the data fell within experimental error for CO_2 concentrations less than 0.13%.

The regeneration time history, depicting CO_2 evolution and purity, for each particle size showed no discernible effect of particle size. CO_2 mass balances were obtained within 2% and measured dry CO_2 contaminants were less than 0.2% for each particle size.

Having established the advantage of the >30 mesh size particles, the moisture content of the sorber was increased to 17 wt % to increase the dynamic CO_2 capacity. The increased moisture content, causing the sorber particles to expand, affected a reduction of the power to mass ratio for the >30 mesh size particles to 4.3 watts per pound CO_2. The <40 mesh size was also tested at the 17%

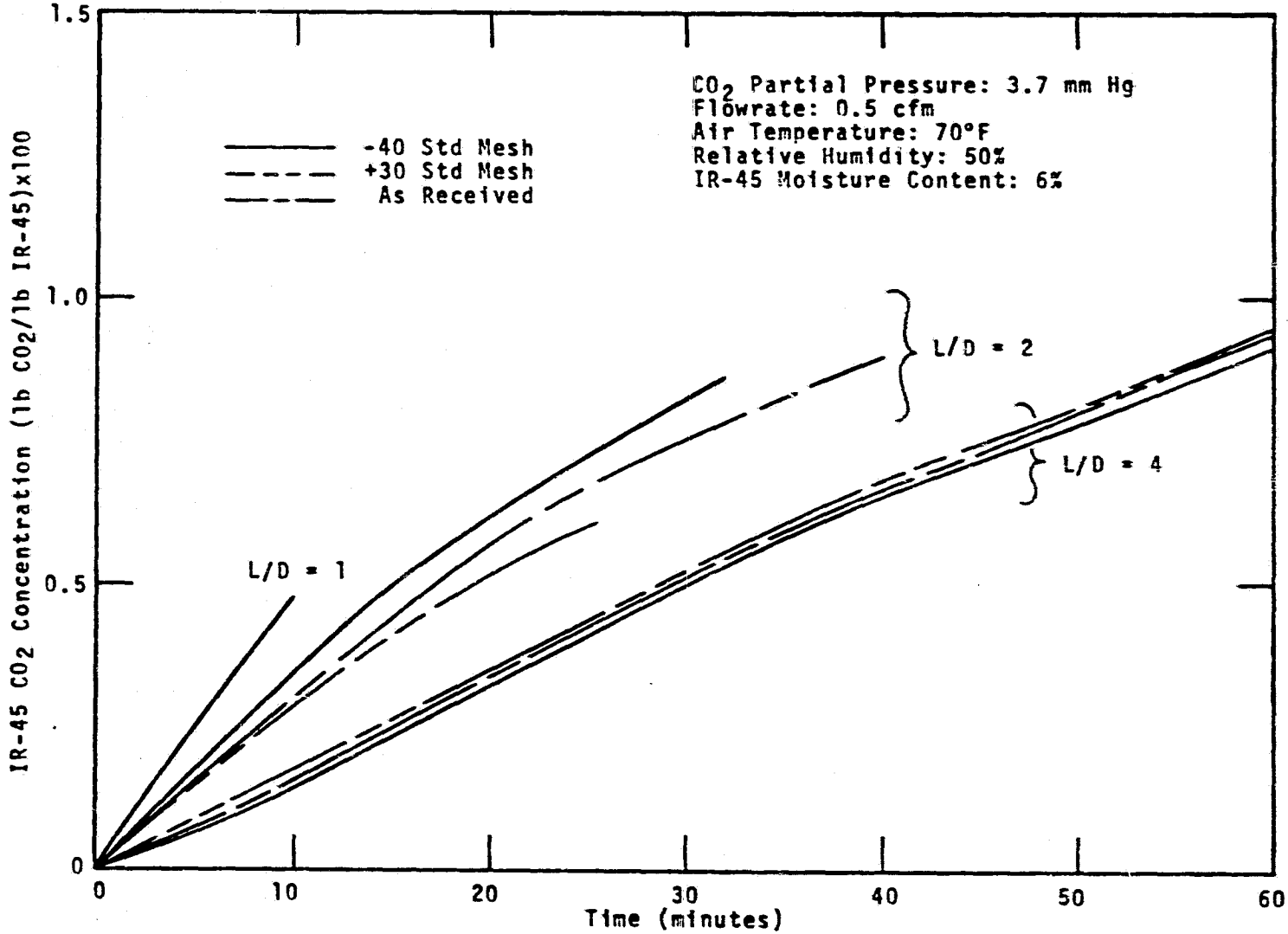

FIGURE 5 BREAKTHROUGH CURVES FOR IR-45

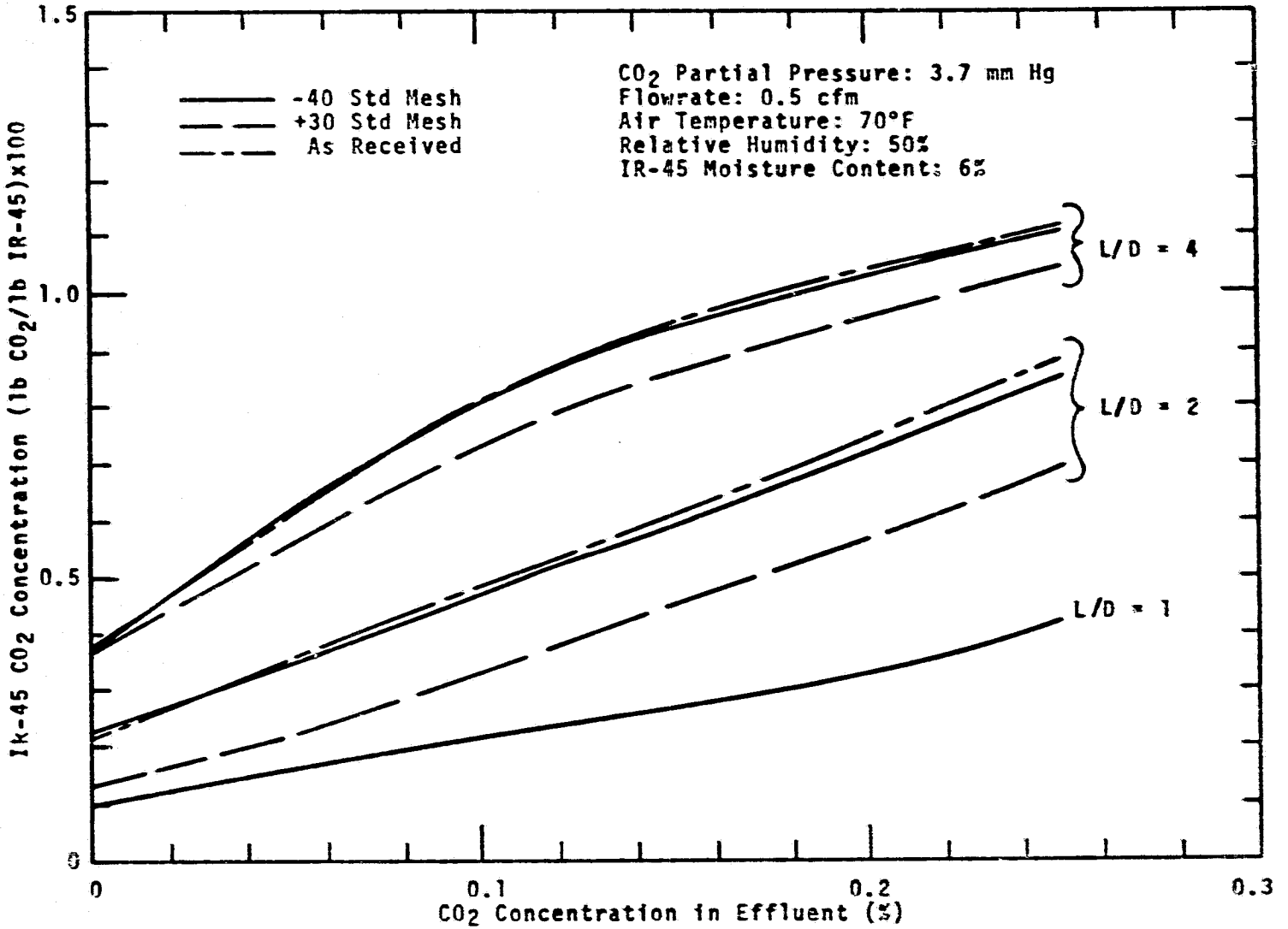

FIGURE 6 BREAKTHROUGH CURVES FOR IR-45

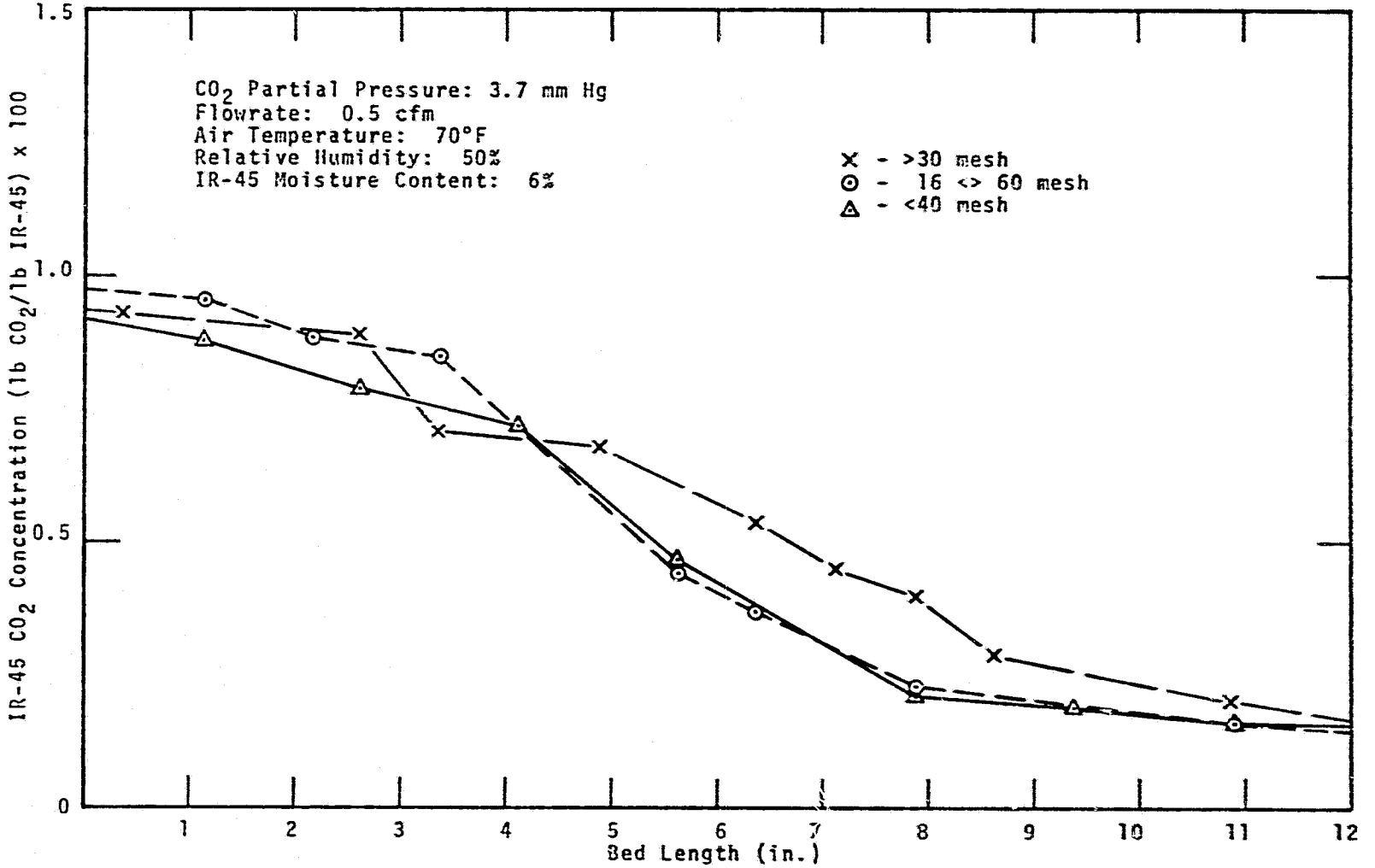

FIGURE 7 CO_2 CONCENTRATION IN IR-45 BED

moisture content with a resulting power to mass ratio of 17.2 watts per pound CO_2 restating the advantage of the >30 mesh size. Further particle size segregation to >20 mesh was rejected on the basis of quantity yield. Using >30 mesh allowed use of 66 wt % of the "as received" material; segregating to >20 mesh would reduce the yield to 19 wt % in turn increasing sorber cost.

Task 1.2 Effect of Process Flow Rate on Sorber CO_2 Capacity and Sorption Efficiency

Increasing the process flow rate through a sorber bed usually increases the fluid phase mass transfer coefficient upon which the sorption efficiency is dependent. The sorption efficiency or fraction of total sorbate sorbed may decrease or be unaffected if:

1. Mass transfer coefficient does not increase with flow rate.

2. Fluid phase mass transfer is not controlling the sorption process.

A mass balance constructed about the process fluid passing through a sorber bed

$$Gdy = Kga(y-y^*)dZ$$

where G ≡ process flow rate ($lb/hr-ft^2$)

y ≡ sorbate concentration in process fluid (lb/lb)

y* ≡ equilibrium sorbate concentration (lb/lb)

Kga ≡ fluid phase mass transfer coefficient ($lb/hr-ft^3$-lb/lb)

dy ≡ differential change of sorbate concentration

dZ ≡ differential sorber bed length

relates the process flow rate to the mass transfer coefficient. The mass balance relationship shows that the change of sorbate concentration (dy) with sorber bed length (dZ) is inversely proportional to the mass transfer coefficient (Kga). Therefore, unless the mass transfer coefficient increases similarly to the process flow rate, the sorption efficiency shall decrease. The CO_2 sorption efficiency and capacity of IR-45, however, are also

effected by the mass and heat transfer associated with the sorber moisture constituent required for optimal CO_2 sorption. Five absorption experiments, excluding CO_2, were performed to ensure that the IR-45 moisture content, post absorption, was within the range for optimal CO_2 sorption. These experiments were performed so that the change of moisture content would not influence the effect of process flow rate.

The experiments for evaluating the effects of process flow rate on sorption efficiency and capacity were performed with IR-45 which contained 15–25 wt % moisture. The >30 mesh particles, determined optimal under Task 1.1, were used in beds exposed to process flow rates from 0.5-3 CFM equivalent to 10-60 fpm space velocities through the sorber bed. The input process air temperature was 70 ± 2°F with a 50-55°F dewpoint and CO_2 partial pressure of 3.7 mm Hg. Unit beds with 1-4 length to diameter ratios containing 0.4-1.5 lbs of IR-45 respectively were used and the experiments terminated when the bed effluent CO_2 partial pressure reached 1.9 mm Hg. The sectioned bed also was used to obtain data relating the sorber CO_2 concentration gradient with process flow rate. The sectioned bed experiments were terminated at absorption times less than, equal to and greater than the bed breakpoint or initial effluent CO_2 detection. This procedure enabled estimating the shape and speed of the mass transfer zone through the sorber bed.

Results.-The data relating process flow rate to the dynamic capacity and sorption efficiency of IR-45 for CO_2 are presented by Figure 8. Data obtained with the 1, 2 and 4 L/D ratio unit beds were reduced to a common parameter; residence time, τ.

$$\tau = L/\bar{U} = V_B/\vartheta$$

where $\tau \equiv$ residence time
$L \equiv$ bed length
$\bar{U} \equiv$ mean space velocity of process fluid through the sorber bed
$V_B \equiv$ sorber bed volume
$\vartheta \equiv$ process volume flow rate

The dynamic capacity related to the residence time is described by relationship

$$\bar{C} = 0.02477 - 0.0088/\tau$$

where $\bar{C} \equiv$ mean CO_2 concentration of sorber for a bed effluent CO_2 partial pressure of 1.9 mm Hg (lb CO_2/lb sorber)

$\tau \equiv$ residence time (seconds)

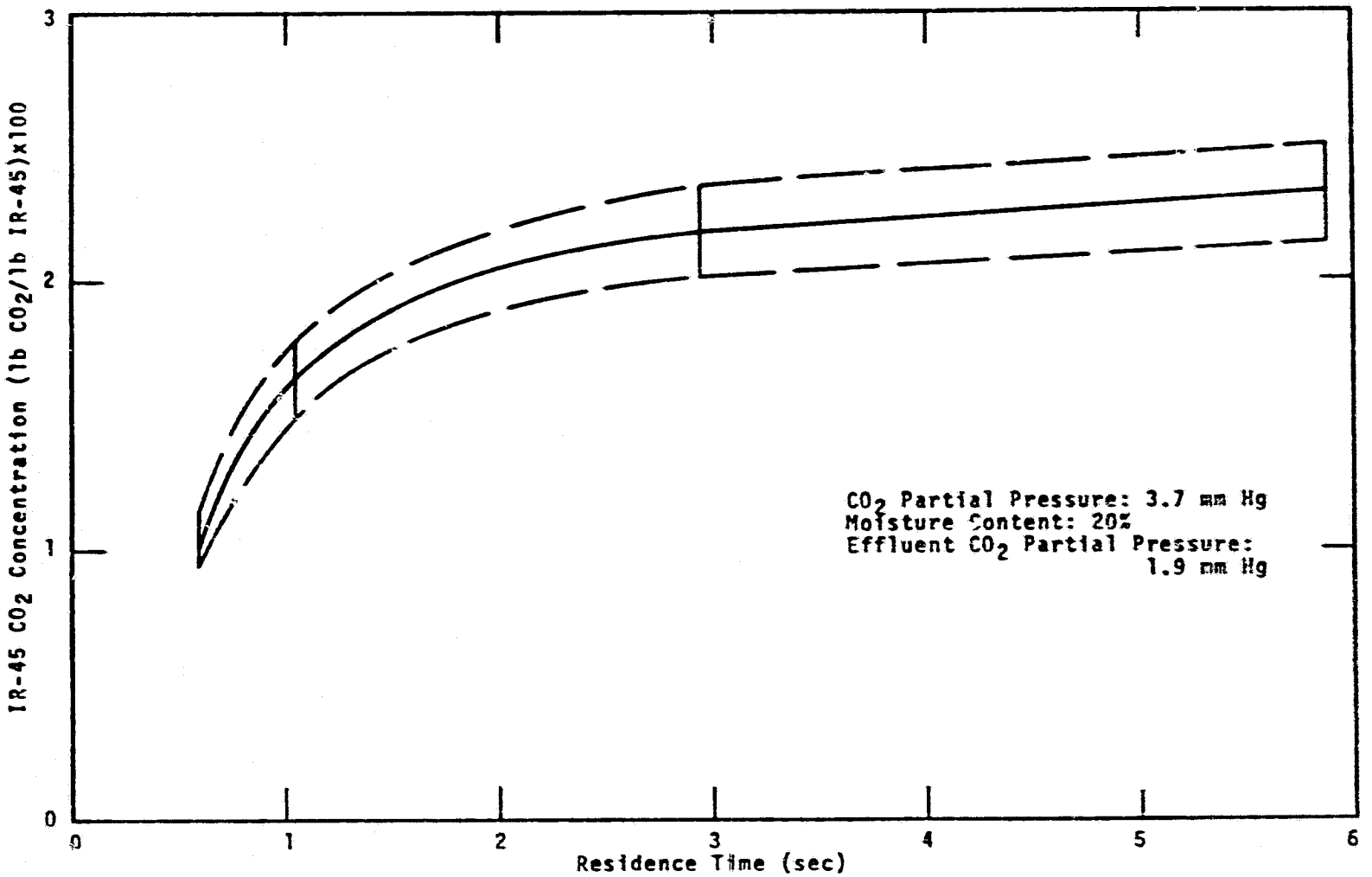

FIGURE 8 IR-45 CO_2 CONCENTRATION RELATED TO RESIDENCE TIME

The data show the sorber CO_2 concentration as 0.019-0.023 lb CO_2/lb sorber for residence times greater than 1.5 seconds; indicating that the dynamic CO_2 capacity of IR-45 is not greatly effected within this residence time range. The sorber CO_2 concentration decreased to 0.010 lb CO_2/lb sorber for a residence time of 0.6 seconds thereby indicating that the sorption efficiency had decreased. The sorption efficiency decreased from 0.86 to 0.75 as the residence time was decreased to 0.6 seconds. These data show that although a period of 0.99 sorption efficiency was maintained before the bed breakpoint the mean sorption efficiency degraded by 14% as the residence time was decreased.

Two process flow rates (46.2; 92.5 lb/hr-ft^2) were used with the sectioned bed for estimating the characteristic mass transfer zone. Figures 9 and 10 illustrate the sorber CO_2 concentration at 1 inch bed increments for different absorption times for each flow rate. The data show the mass transfer zone totally within and leaving the sorber bed. For both flow rates used for these experiments, the mass transfer zone was approximately 3.1 inches long. The bed breakpoint times obtained with the unit bed and sectioned bed were compiled and the apparent speed of the mass transfer zone is shown related to the process flow rate by Figure 11. The data exhibit a linear relationship of the apparent mass transfer zone speed to the process flow rate. This relationship may be described by

$$S = a + bG$$

where $S \equiv$ mass transfer zone speed (ft/hr)
$G \equiv$ process flow rate (lb/hr-ft^2)

The effect of the process flow rate on sorber moisture content was determined by observing the change of weight of the sectioned bed cells. These experiments indicated a reduction of the moisture content of the sorber for 1.5 inches, measured from the inlet, to 12 wt % for a process flow rate of 226 lb/hr-ft^2 and a 60 minute absorption time. Since even for these experiments the mean sorber moisture content was within the range for optimal CO_2 sorption, the influence of moisture content was alleviated.

Task 1.3 Pressure Drop Through IR-45

Throughout the experiments for studying the effect of sorber particle size and process flow rate, the sorber bed pressure drop was monitored both for sorber containing 6 wt % moisture and 15-25 wt % moisture.

Results.-The pressure drop data are presented by Figure 12 which shows the unit pressure drop (in. H_2O/ft bed) and process flow rate (lb/hr-ft^2) for three particle sizes of sorber with 6 wt % moisture content and the >30 mesh particles with 20 wt% moisture

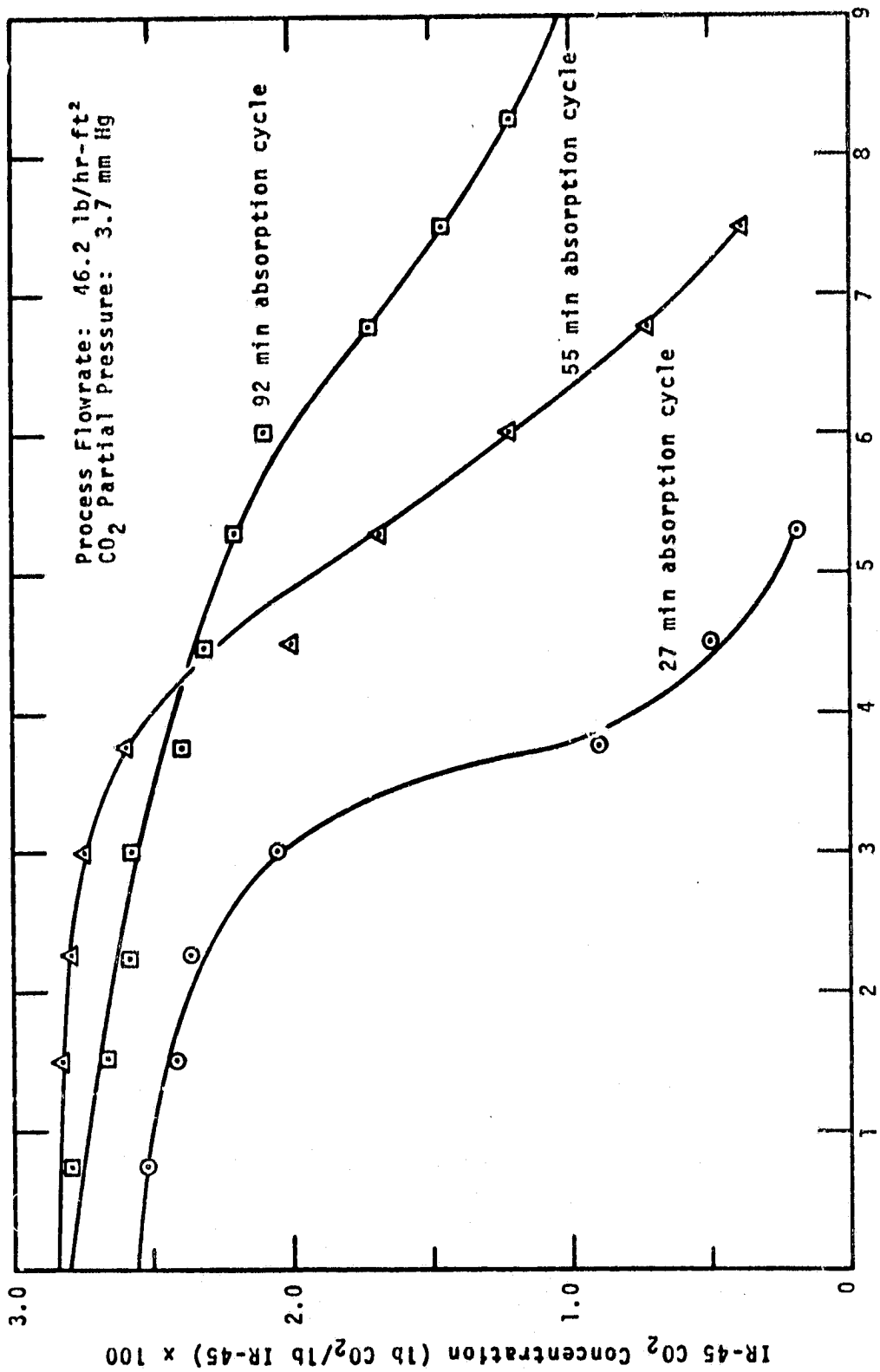

FIGURE 9 CO_2 CONCENTRATION IN IR-45 BED

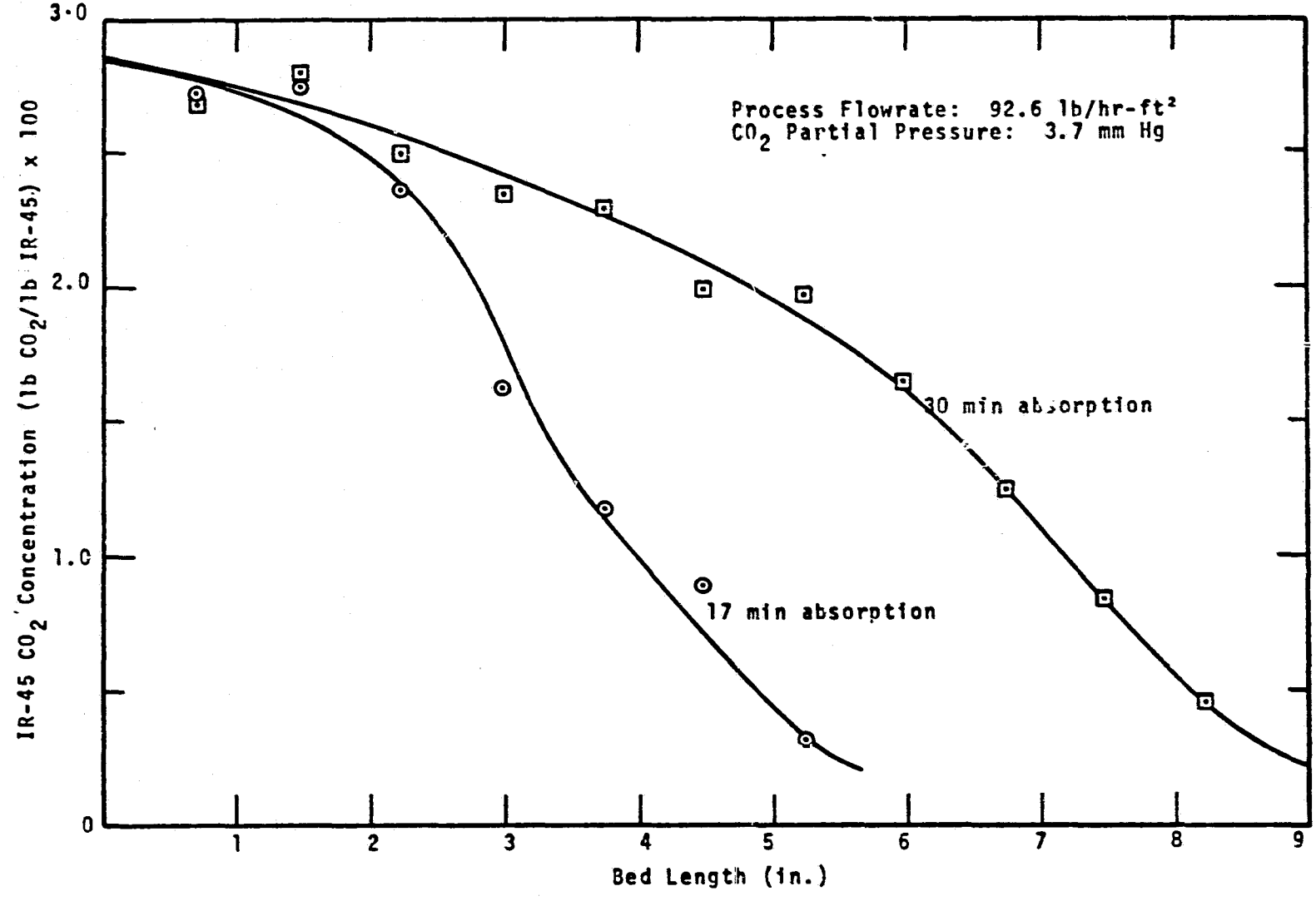

FIGURE 10 CO_2 CONCENTRATION IN IR-45 BED

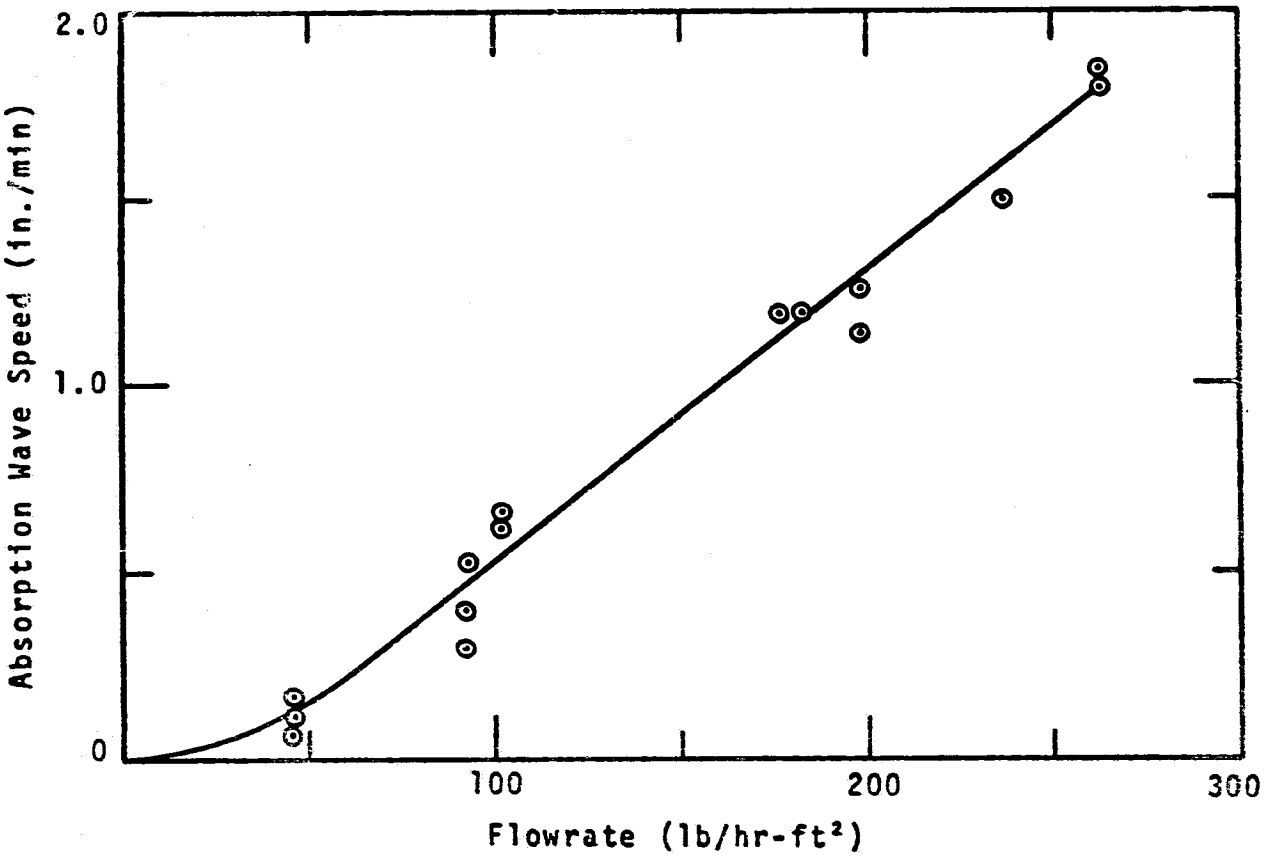

FIGURE 11 ABSORPTION WAVE SPEED AND FLOWRATE

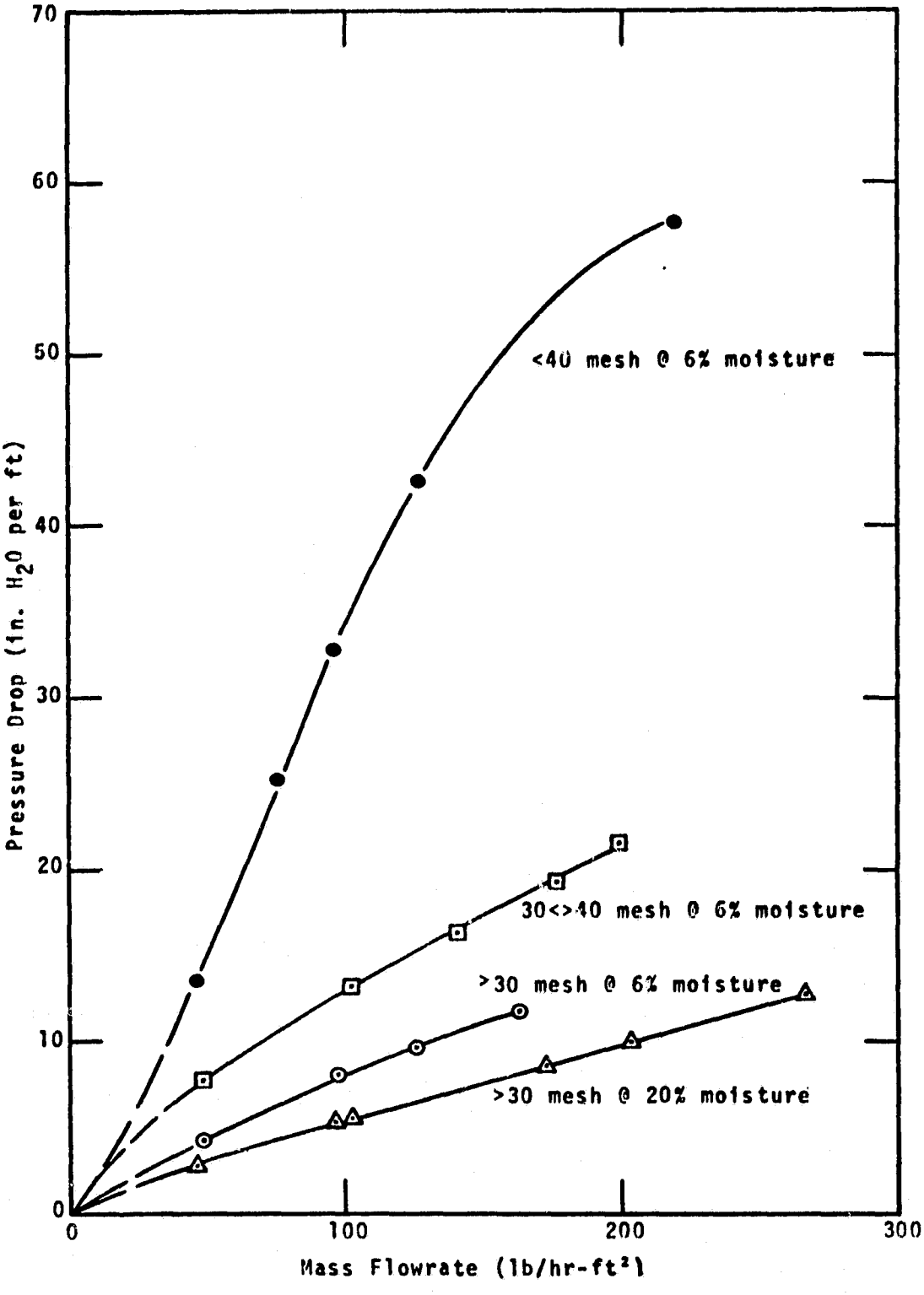

FIGURE 12 PRESSURE DROP OF IR-45

content. For the >30 mesh particles with 6 wt % moisture content, a unit pressure drop of 10.1 in. H_2O/ft was observed at a 150 lb/hr-ft^2 flow rate. The corresponding unit pressure drop for sorbet with 20 wt % moisture content was 7.6 in H_2O/ft; a reduction of about 25%. The decrease of pressure drop with increased moisture content is attributed to particle expansion causing the packing density to decrease. The beds used for this work were constrained; the pressure drop through an unconstrained bed would not exhibit the significant increase with moisture content reduction since the packing density would be established by the momentum of the process fluid; in fact, as the particles became drier fluidization could occur.

Task 1.4 IR-45 Pretreatment Evaluation

The manufacturing process of IR-45 includes the use of organic solvents which during regeneration of "as received" IR-45 may be desorbed from the IR-45 and contaminate the concentrated CO_2 and carry over into the process stream during the initial minutes of the absorption cycle. Also, the desorbed solvents could contribute to the presence of an odor in the process stream.

The objective of this task was to evaluate some techniques to remove the desorbable trace organics by subjecting the IR-45 to a pretreatment which would not influence the CO_2 capacity of IR-45. Pretreatment processes investigated were Soxhet type extraction using acetone and methyl alcohol. Approximately 5 lb batches of >30 mesh IR-45 were treated by Soxhet extraction. This process involves (1) vaporizing the extractant, (2) condensing the extractant on the IR-45 and (3) returning the condensed extractant along with the impurities to the extractant boiler where the impurities are accumulated. Following 24 hours of exposure, the IR-45 was dried in a vacuum oven maintained at >5 mm Hg and 160°F. The vacuum oven temperature was then increased to 215°F and the IR-45 dried for an additional 48 hours. The effect of the pretreatment was then evaluated by placing approximately 200 grams of IR-45 into a clean sealed container and allowing the IR-45 to set for 120 hours. The gas above the IR-45 was then analyzed by gas chromatograph and compared to similar exposure of "as received" IR-45. Also, during the absorption-regeneration cycling of the pretreated IR-45 the regeneration condensate and effluent process air was analyzed and compared to "as received" IR-45 regeneration condensate and process air. Gas chromatography and ultraviolet spectrophotometry were used for the gas and water analyses.

The absorption-regeneration cycling performed on the pretreated IR-45 for pretreatment effect on CO_2 was done with 75-80°F/50% RH air, 1 CFM flow rate, 3.7 mm Hg CO_2 partial pressure and 750 mm Hg total pressure.

Results.-Analysis of the "as received" regenerated IR-45 process air identified toluene as the primary (90%) contaminant. Toluene concentrations ranging from 9,000-14,200 $\mu g/m^3$ were found present in the process air. The remaining 10% of the contaminants were not isolated by chromatographic analysis. Also, a 30 gram sample of "as received" IR-45 was placed under a 50 cc/min nitrogen purge and the sample incrementally heated to 190°F over a period of 162 hours. The effluent nitrogen purge was periodically analyzed by gas chromatography. Several off-gas constituents were observed with toluene dominating. As the test continued the unidentified constituent concentrations were reduced while the toluene remained. Table 3 presents the concentration of toluene in the effluent nitrogen purge along with time and sample temperature.

TABLE 3 - TOLUENE CONCENTRATION IN EFFLUENT NITROGEN PURGE OF "AS RECEIVED" IR-45

Total Time (hours)	Temperature (°F)	Toluene Concentration ($\mu g/m^3$)
0.25	76	72
1.0	190	260
2	180	14,200
17	175	990
20	175	590
25	190	210
90	160	12
114	160	168
138	160	392
162	170	213

The effectiveness of acetone extraction to reduce the "as received" contaminant level was not determined because of the concentration of acetone in the regenerated IR-45 process air. Although the acetone extracted IR-45 was exposed to 200°F during drying, acetone concentrations as large as 75 mg/m^3 were detected. Because of the evident difficulty associated with the acetone, the methyl alcohol pretreatment was subsequently evaluated. Analyses of the methyl alcohol treated IR-45 regeneration process air yielded a toluene concentration of 112 $\mu g/m^3$ while the regeneration condensate contained 20-44 ppm by weight of toluene. Although the methyl alcohol pretreatment reduced the toluene concentration the odor associated with IR-45 remained. However, upon exposure of IR-45 to absorption-regeneration cycling the odor became undetectable.

Samples weighing 1.5 lb of methyl alcohol treated IR-45 were exposed to continuous cyclic absorption-regeneration. Figure 13 presents absorption data showing the sorber bed effluent CO_2 concentration for "as received" and methyl alcohol treated IR-45 and absorption time. These data are for the initial and eleventh absorption cycles. The eleventh absorption cycle of the methyl alcohol treated IR-45 shows a decrease of absorption efficiency compared to the "as received" IR-45. After completion of the fourteenth cycle, during which practically no CO_2 was absorbed, the IR-45 was weighed and found to contain 36.5% moisture. Similarly, the "as received" IR-45 contained 35.8% moisture. The absorption efficiency degradation was attributed to the increasing moisture content and not the pretreatment.

A pretreatment used to regenerate ion exchange resins in water purification applications was also performed on the IR-45. IR-45 was exposed to a cyclic wash consisting of 4% HCl, 4% NaOH, and then water rinse at both ambient and 160-170°F temperatures. After treatment, the resin was dried and a sample exposed to an absorption cycle. The dynamic CO_2 capacity of acid-base treated IR-45 was 0.009-0.015 lb CO_2/lb IR-45 compared to 0.023 lb CO_2/lb IR-45 for "as received" IR-45. The decrease of CO_2 capacity and range of values indicated that the acid-base treatment degraded the IR-45 CO_2 capacity. Comparison of contaminant reduction of the acid-base treatment was not performed after observing the reduction of CO_2 capacity.

Task 1.5 Effects of Steam Flowrate on IR-45 Regeneration

The sorber regeneration process is particularly important for systems which remove and concentrate CO_2 for further use. Saturated or superheated steam at temperatures from 180 to 225°F enters the IR-45 bed and condenses on the cool IR-45 particles. Initially, the bed void volume air is displaced by the entering steam while CO_2 is desorbed from the heated IR-45 and reabsorbed by the remaining cool portion of the bed. As regeneration continues, further displacement of void volume air occurs, CO_2 is desorbed and reabsorbed until the CO_2 partial pressure and unregenerated IR-45 CO_2 concentration are in equilibrium and no further absorption occurs. Thereafter, CO_2 exits the IR-45 bed driving the residual void air before it until the entire bed is regenerated and steam breaks through the bed. Since the final IR-45 to be regenerated is saturated with CO_2 at a partial pressure essentially equal to the steam pressure, complete regeneration is required for efficient CO_2 concentration.

The performance of the steam regeneration process to concentrate maximum purity CO_2 depends upon the chromatographic separation of the bed void air, desorbed CO_2 and the steam front. This separation may be influenced by sorber particle size, bed configuration, available CO_2 and steam flow rate. Small sorber particles would be

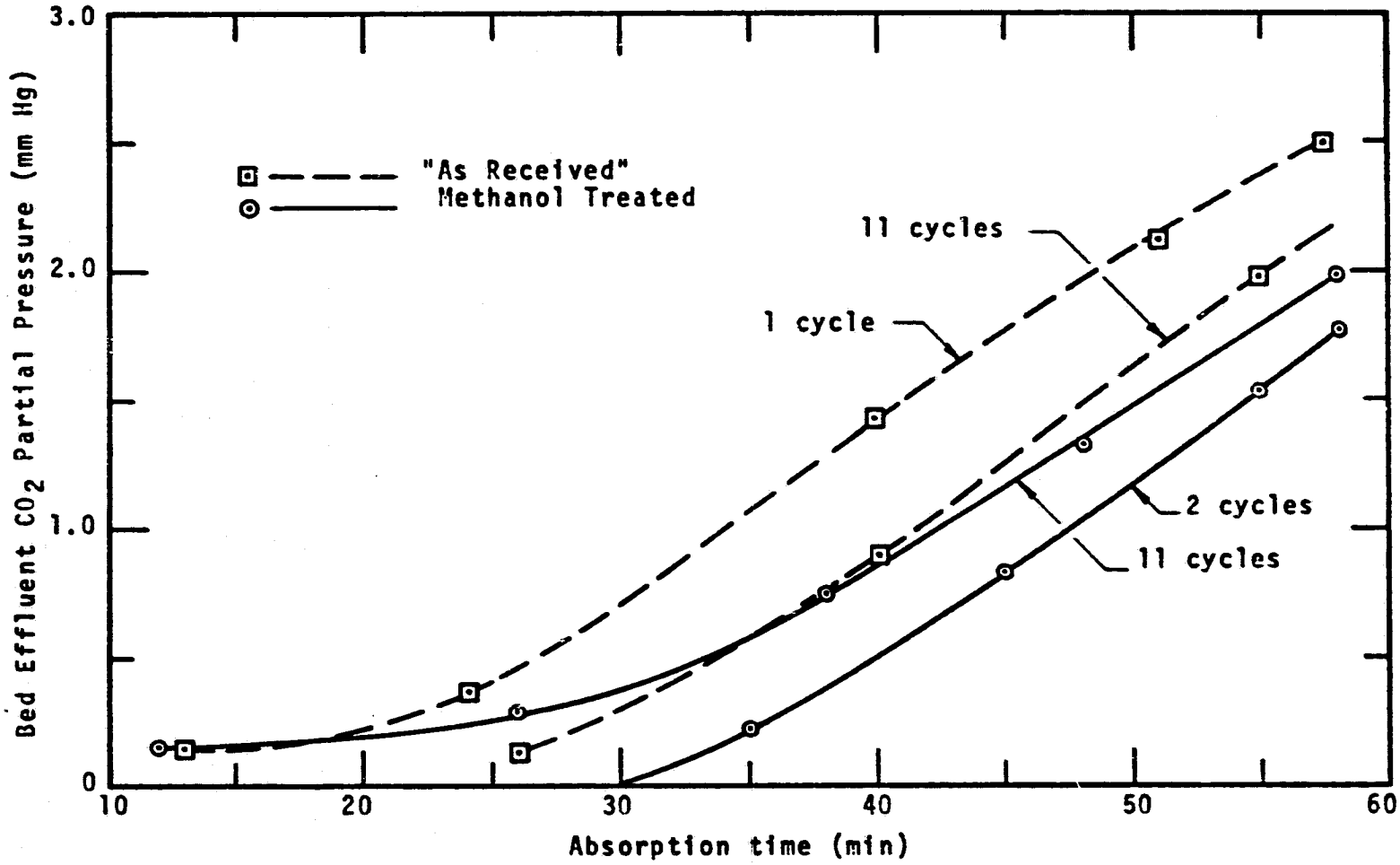

FIGURE 13 PRETREATED AND "AS RECEIVED" IR-45 ABSORPTION CYCLE

expected to increase the number of mass transfer units effecting CO_2 absorption and reduce bed void volume. The sorber CO_2 concentration effects the CO_2-air-steam separation if the quantity of CO_2 required to drive the final void air from the bed was large compared to the available CO_2. Also, since the bed must be completely regenerated the power required to concentrate a unit quantity of CO_2 increases as the available CO_2 decreases. Particles of <40 mesh and >30 mesh were regenerated and the air-CO_2 separation compared to determine if an advantage for increasing the CO_2 purity was available. The effect of steam flowrate, within the range of 0.11 to 0.38 lb/hr, was evaluated for regeneration rate, heating efficiency and CO_2-air separation. Beds of 2 and 4 L/D ratios were used to determine if bed configuration effected the concentration of maximum purity CO_2.

Results.-Figure 14 illustrates the response of the Beckman Model 668 oxygen probe used to indicate the CO_2-air separation. The CO_2-air separation affected by <40 mesh and >30 mesh IR-45 particles is shown by Figure 15. For these experiments 1.5 lb of the respective particle sizes containing 0.016 ± .001 lb CO_2/lb IR-45 were regenerated in 3.0 in. diameter beds with a steam flow rate of 0.37 lb/hr. The data show a decrease of O_2 concentration in the regeneration effluent occurring about 19 minutes into the regeneration for both particle sizes. The oxygen concentration decreased to less than 1% in 24 minutes for each particle size. The CO_2-air separation characteristics of both particle sizes are similar and no significant advantage exhibited with respect to particle size.

Figure 16 presents data showing the effect of steam flowrate on regeneration rate and Figure 17 presents the complimentary regeneration effluent flowrate for the data of Figure 16. Beds with 1.54 lb of IR-45 with 20% moisture content and 0.020 ± .002 lb CO_2/lb IR-45 were exposed to 0.11 and 0.33 lb/hr steam flowrates for these tests. The total regeneration times required with the 0.11 lb/hr steam flowrate were 116-122 minutes while the 0.33 lb/hr steam flowrate enabled the same quantity of IR-45 to be regenerated in 35-37 minutes. Regeneration with 0.11 lb/hr steam flowrate required 0.142 lb steam/lb IR-45; with 0.33 lb/hr steam flowrate 0.129 lb steam/lb IR-45 was required. On a dry basis these values increase to 0.177 and 0.161 lb steam/lb dry IR-45 respectively.

Regeneration tests were performed on IR-45 with 6% moisture content. The tests were performed with two beds (L/D = 2 and 4). and steam flowrates of 0.30 to 0.38 lb/hr. The beds contained 0.77 and 1.52 lb of sorber with a CO_2 concentration of 0.008 ± .0002 lb CO_2/lb IR-45. Figure 18 presents regeneration data for both beds. The data show that a regeneration time of 33 to 37 minutes was required for the L/D = 4 bed with a steam flowrate of 0.38 lb/hr. The steam required for regeneration was 0.146 to 0.164 lb steam/lb

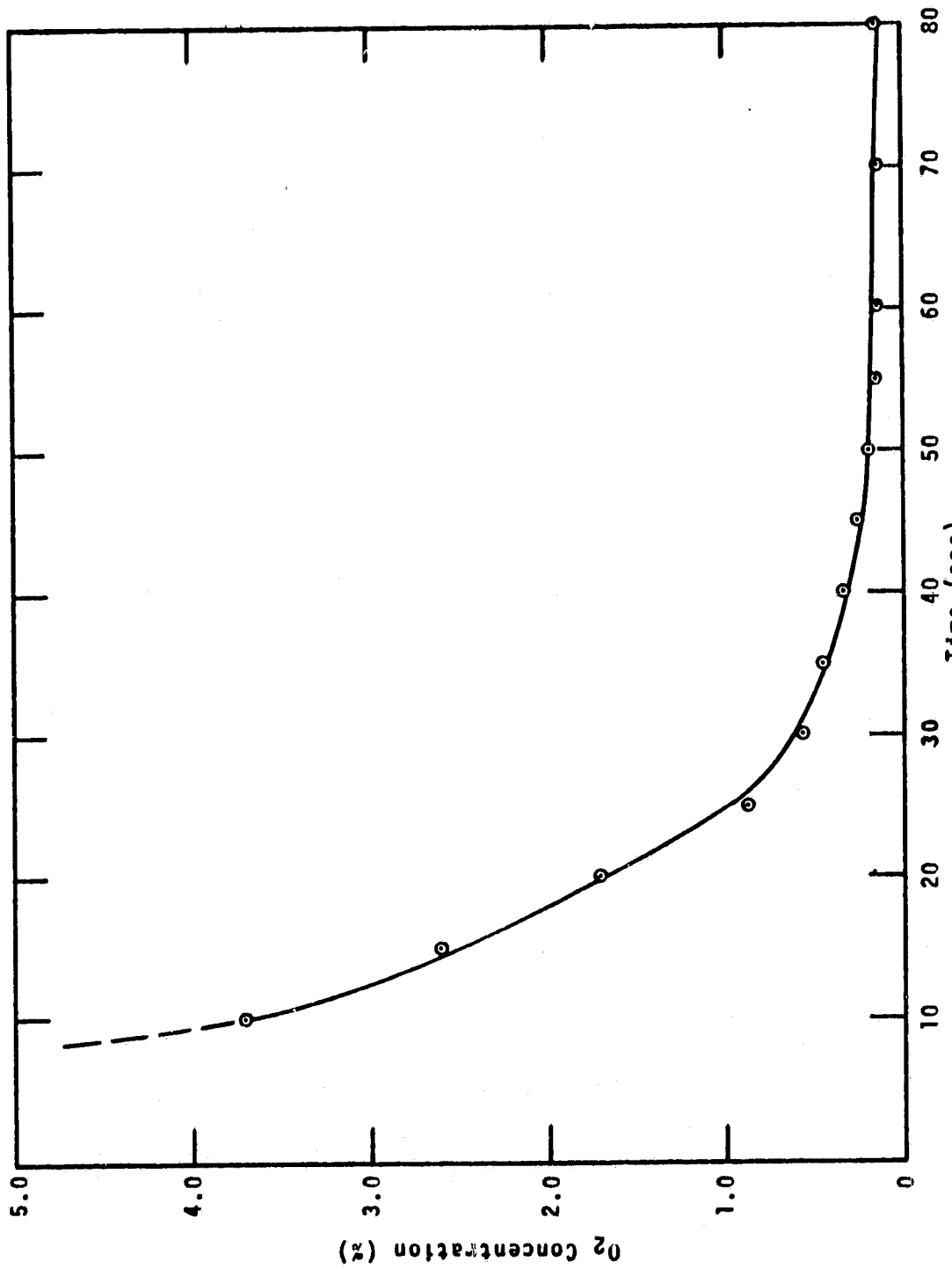

FIGURE 14 CO_2-AIR SEPARATION TRACING OXYGEN

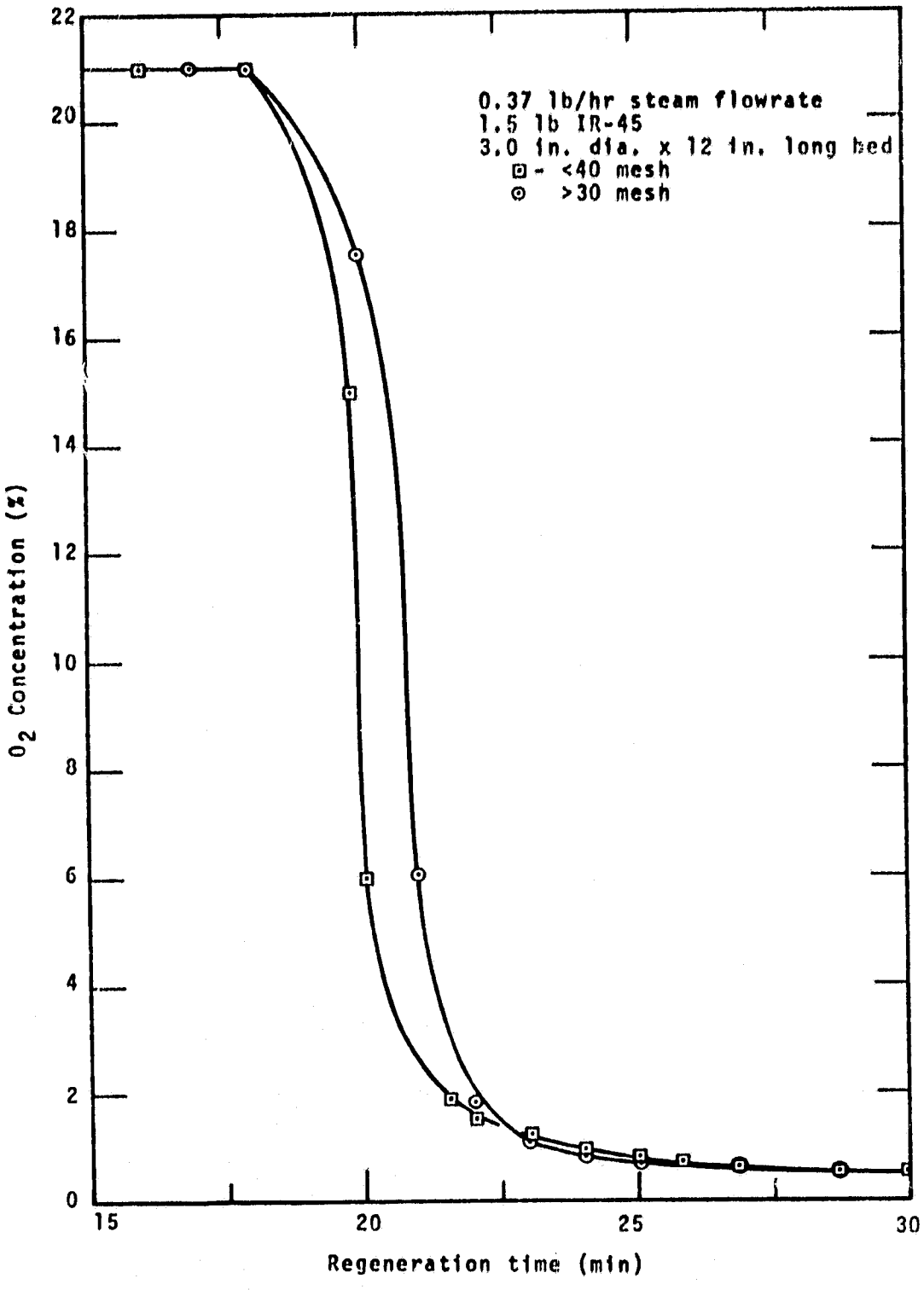

FIGURE 15 PARTICLE SIZE EFFECT ON CO_2 SEPARATION

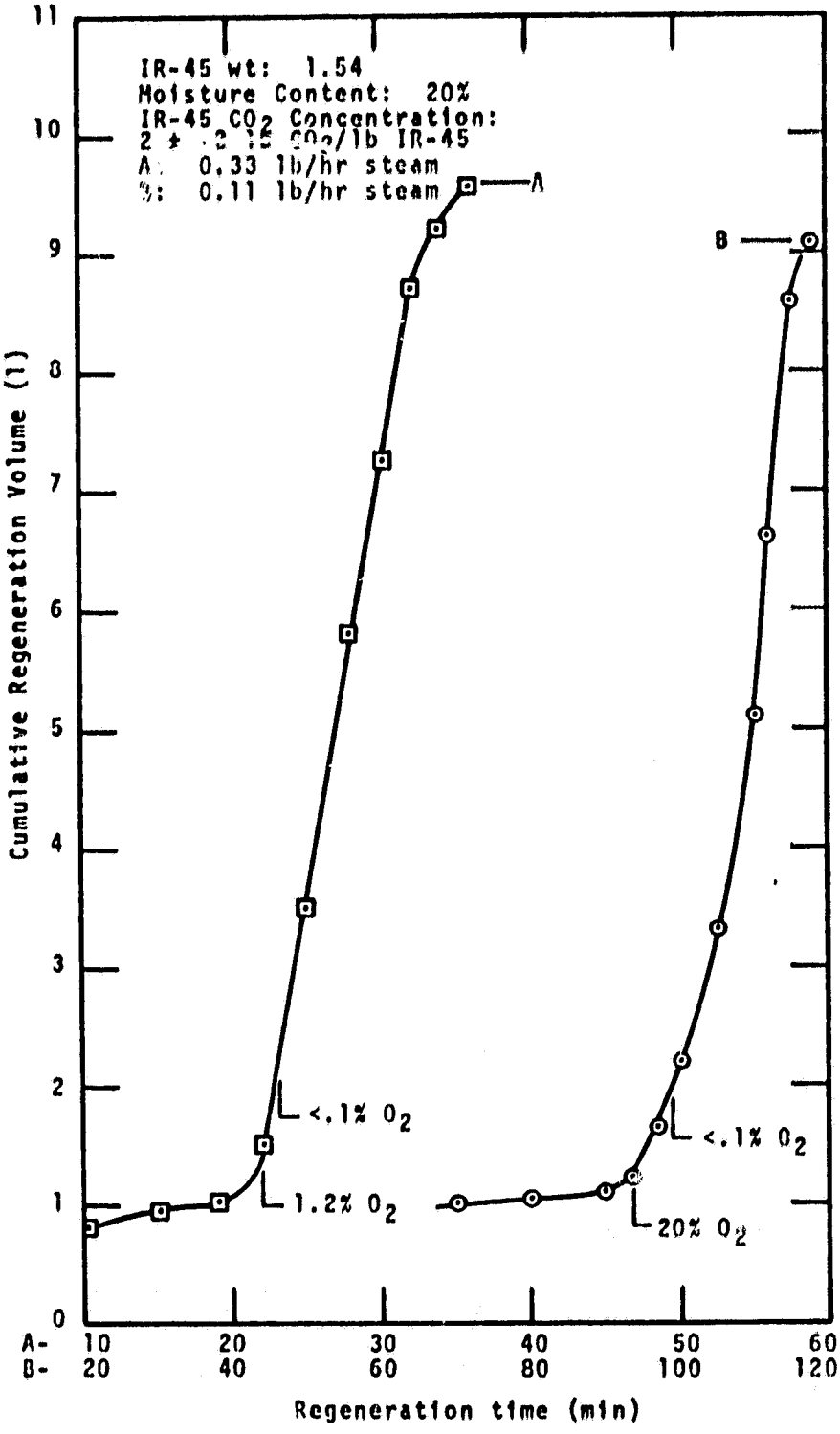

FIGURE 16 EFFECT OF STEAM FLOWRATE ON REGENERATION

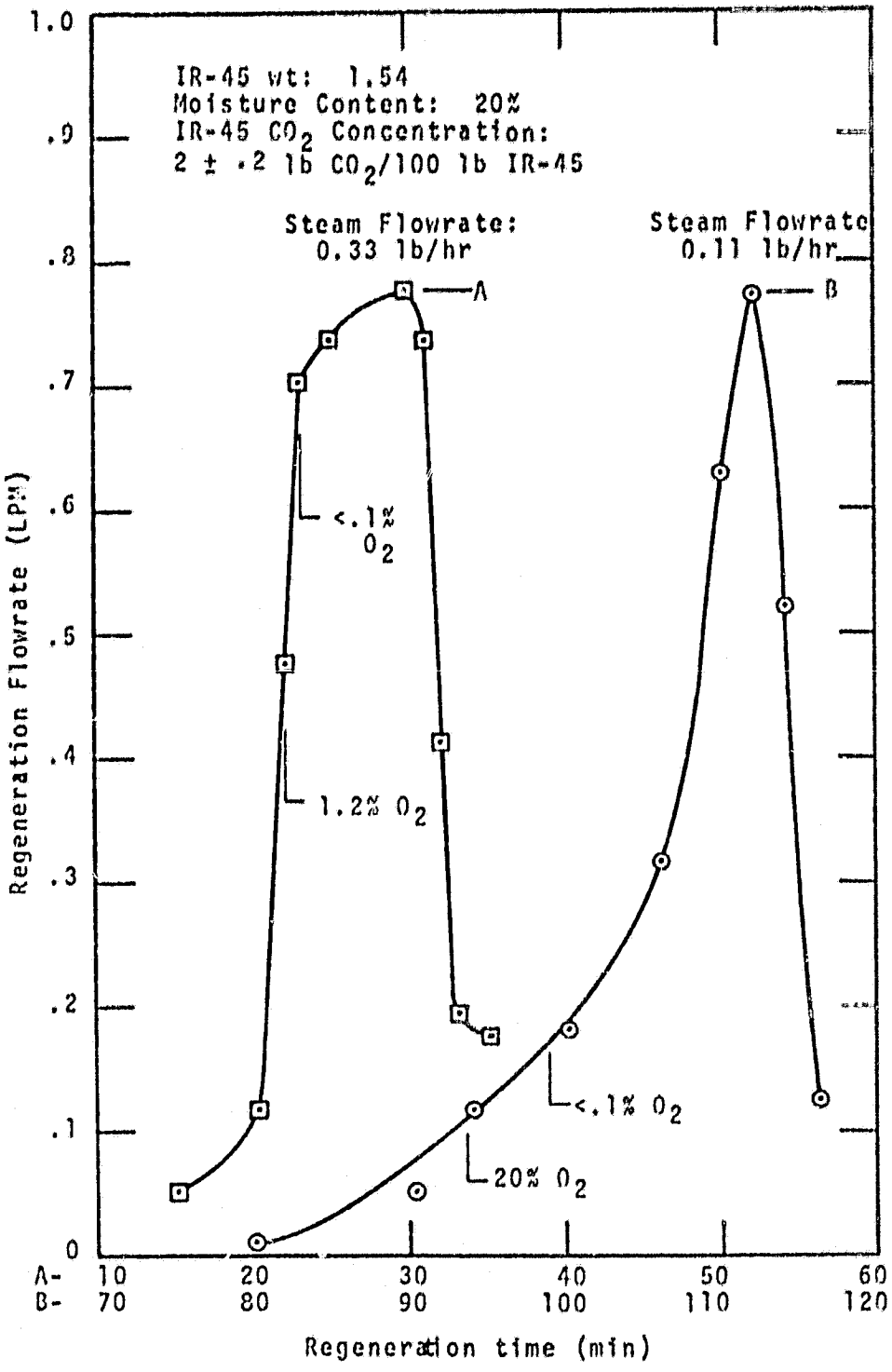

FIGURE 17 STEAM FLOWRATE EFFECT ON GAS FLOWRATE

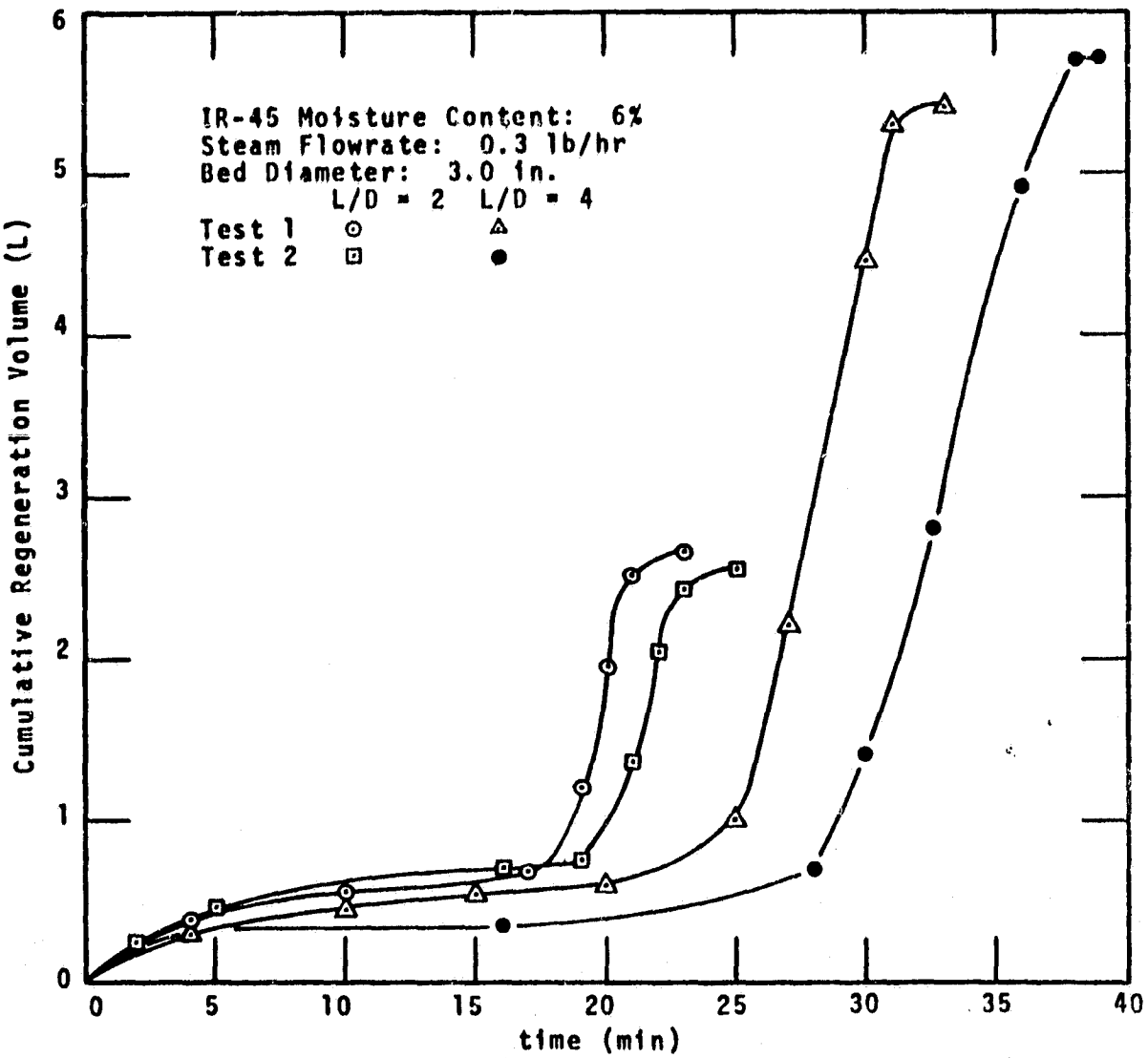

FIGURE 18 REGENERATION OF IR-45 BEDS

dry IR-45. Tests with the L/D = 2 bed showed that 23 to 25 minutes was required for regeneration with a steam flowrate of 0.32 lb/hr. A steam requirement of 0.152 to 0.162 lb steam/lb dry IR-45 was obtained for these tests.

Noted on Figures 16 and 17 are points at which mass spectrometer samples were taken of the regeneration effluent. The CO_2-air separation occurred as the effluent flowrate increased indicating the desorption of CO_2. The regenerations performed with 0.33 lb/hr steam flowrate show that <0.1% O_2 was present for an effluent flowrate of 0.7 lpm (0.024 cfm) while the 0.11 lb/hr steam flowrate showed that <0.1% O_2 was present for 0.17 lpm (0.006 cfm) effluent flowrate. Also, the data show that more of the contaminant CO_2 is evolved at higher flowrates for the 0.33 lb/hr steam flowrate than for the 0.11 lb/hr steam flowrate. Separation of the CO_2 and steam front occurred rapidly as the regeneration effluent flowrate became less than 0.15 lpm. This separation occurred for both the 0.11 and 0.33 lb/hr steam flowrate which indicated that within the range of steam flowrates and beds used the CO_2-steam separation is not effected by these parameters.

Figure 19 shows the regeneration time and cumulative volume for the regeneration of beds with L/D = 3.9/1 and 2.2/1 at the same steam flowrate. Desorption of CO_2 began in approximately 11 and 20 minutes and the steam requirement for complete regeneration was 0.168 and 0.161 lb steam/lb dry IR-45, respectively for the beds. CO_2-air separation occurred similarly for both beds showing no significant dependence of CO_2 purity on bed L/D.

Task 1.6 Effect of High CO_2 Partial Pressures on Absorption

Several absorption tests were performed with CO_2 partial pressures of 0.8-15 mm Hg. These tests were conducted with 75-80°F air temperatures, 50-55°F dewpoints, 0.5-1.0 CFM flowrates and 18-20% sorber moisture content to determine the effect of CO_2 partial pressure on the dynamic CO_2 capacity and sorption efficiency of IR-45. Sorber beds with 2 and 4 L/D were used and the absorption test terminated when the sorber bed effluent CO_2 concentration equaled the input concentration.

Results.-Figure 20 presents the dynamic saturation capacity of IR-45 as a function of CO_2 partial pressure. The saturation capacity was determined to be inversely related to the CO_2 partial pressure within the range of investigation. The data show a 2% saturation capacity for a CO_2 partial pressure of 1 mm Hg and increases to 2.7% at 4 mm Hg CO_2 partial pressure. The saturation capacity of IR-45 with 20% moisture content is expressed:

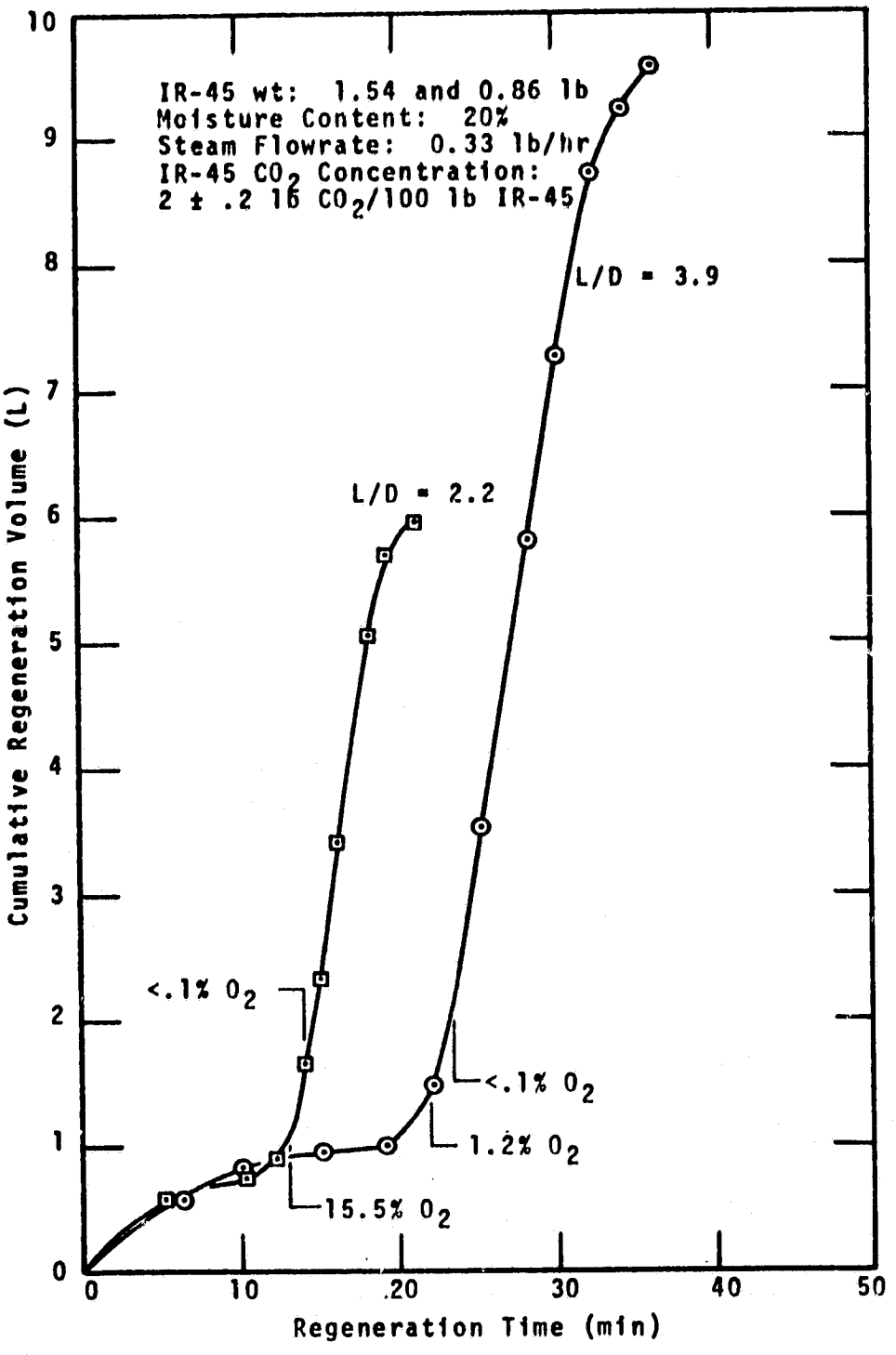

FIGURE 19 BED LENGTH EFFECT ON REGENERATION

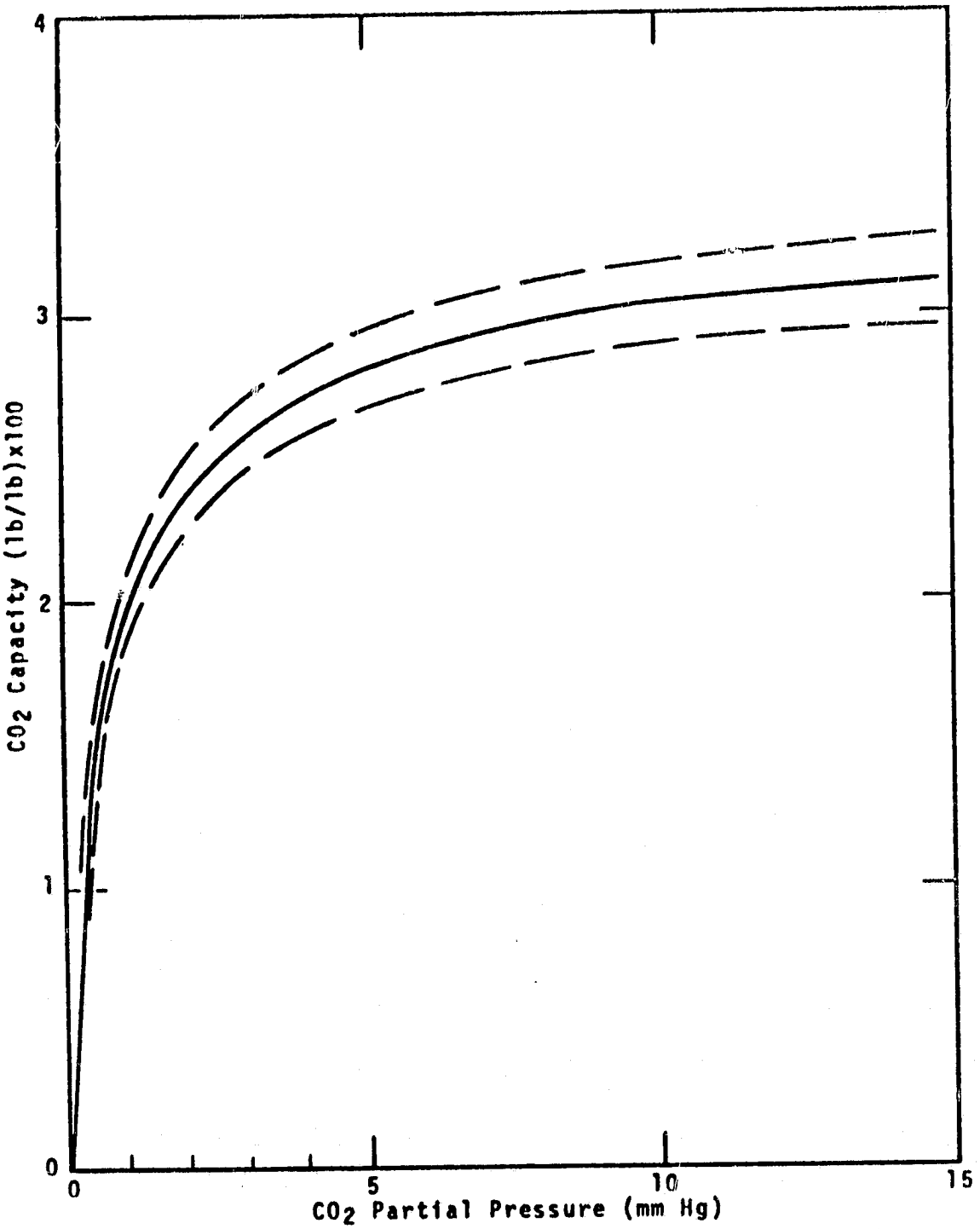

FIGURE 20 IR-45 CO_2 CAPACITY-CO_2 PARTIAL PRESSURE

$$\ln X^* = a + b/\sqrt{P_{CO_2}}$$

where X^* = capacity (percent)
P_{CO_2} = CO_2 partial pressure (mm Hg)

a = 1.2767
b = -0.587

Task 1.7 Effects of 1, 2 and 3 Bed Design

The energy requirement of the IR-45 polymeric, steam regenerated, CO_2 concentration system is primarily effected by the steam regeneration process. Maximizing the quantity of CO_2 absorbed per unit weight of IR-45 permits minimizing the energy required to concentrate a unit weight of CO_2. Task 1.7 included evaluating the results obtained during Tasks 1.1-1.6 to project the energy requirements of 1, 2 and 3 bed system designs. CO_2 capacity, concentrated CO_2 purity and system simplicity associated with each type of system design were also evaluated. Single bed (L/D's= 4 and 2/1) absorption and regeneration characteristics were reduced to provide the CO_2 capacity, purity and energy information for 1 and 2 bed system designs. The sectioned bed results were used to provide CO_2 capacity information for the 3 bed (L/D = 2/1) series system design. A regeneration steam flowrate of 0.33 lb/hr was used for each system design.

Results.-Table presents the 1, 2 and 3 bed system design comparison data. These data were applied to the single and multibed system designs by determining the energy expended during absorption and concentration of one pound of CO_2 for 3 process flowrates.

TABLE 4 - 1, 2 AND 3 BED SYSTEM COMPARISON

	1	2	3
Bed weight (lb)	1.54	0.77	0.77
Process Flowrate, (lb air/ hr-ft^2-lb IR-45)	30,60,120	60,120,240	60,120,240
Half Life CO_2 capacity* (wt %)	2.3,2.2,1.8	2.2,1.7,1.3	2.5,2.5,1.9
Steam flow rate (lb/hr-lb IR-45)	.214	.428	.428
Pressure drop (in. H_2O)	3,6,9	1.5,3,4.5	1.5,3,4.5
Absorption time (min)	140,68,32	71,28,13	71,28,13
Regeneration time (min)	36,36,36	21,21,21	21,21,21

* Determined when effluent concentration equals 1/2 inlet concentration

1-Bed System Design: A bed containing 1.54 lb IR-45 was exposed to process flowrates of 46.2, 92.6 and 185 lb/hr-ft^2 and permitted to absorb CO_2 until the bed effluent CO_2 partial pressure attained 1.9 mm Hg; bed half-life. The energy expended for this absorption was calculated from the bed pressure drop, process flowrate and absorption time and resulted in 40.6, 82 and 143 Btu/lb CO_2 for the respective process flowrates. The regeneration energy was calculated directly from the steam flowrate and regeneration time. The regeneration energies for the three process flowrate absorptions were: 5420, 5650 and 6930 Btu/lb CO_2. The concentrated CO_2 purity was considered 98% and greater for a 95% recovery as obtained from the regeneration CO_2-air separation data.

2-Bed System Design: The 2-bed system design evaluation was performed for 2 beds each containing 0.77 lb IR-45 and exposed singularly to 46.2, 92.6 and 185 lb/hr-ft^2 process flowrates. In the same manner as the 1-bed design, the absorption energies determined were: 36.5, 48.9 and 81 Btu/lb CO_2. The regeneration energies were: 6610, 8530 and 11,120 Btu/lb CO_2.

The increase of regeneration energy of the 2-bed system compared to the 1-bed system is due to the decrease of CO_2 capacity observed as the process flowrate increased.

3-Bed System Design: Considered also was a 3-bed design in which 2 beds would be absorbing in series while the third bed was regenerated. The sectioned bed studies, performed in Task 1.2, indicated that regenerating only the input section of a bed which had absorbed to its breakpoint would provide an increase of regeneration efficiency since the input section is nearly saturated (2.5 wt %) with CO_2. The output section of the bed would be exposed to further absorption. With this consideration, the regeneration energy required for a 0.77 lb IR-45 bed was determined to be 4985, 5780 and 7560 Btu/lb CO_2 for the 46.2, 92.6 and 185 lb/hr-ft^2 process flowrates.

Figure 21 presents the concentration energy per lb CO_2 related to process flowrate per lb IR-45 for the 1,2 and 3-bed system designs.

Regarding system simplicity, the single bed system design would basically require a timer control for the absorption cycle and a time or flowrate control for regeneration. Three-way valves upstream and downstream of the bed would switch to emit steam for regeneration and CO_2 concentration or process flow for CO_2 absorption. During regeneration, the bed void volume air would be returned to the cabin and upon desorption of CO_2 the downstream valve, controlled either by a time or flowrate signal, would switch to pass CO_2 to the accumulator.

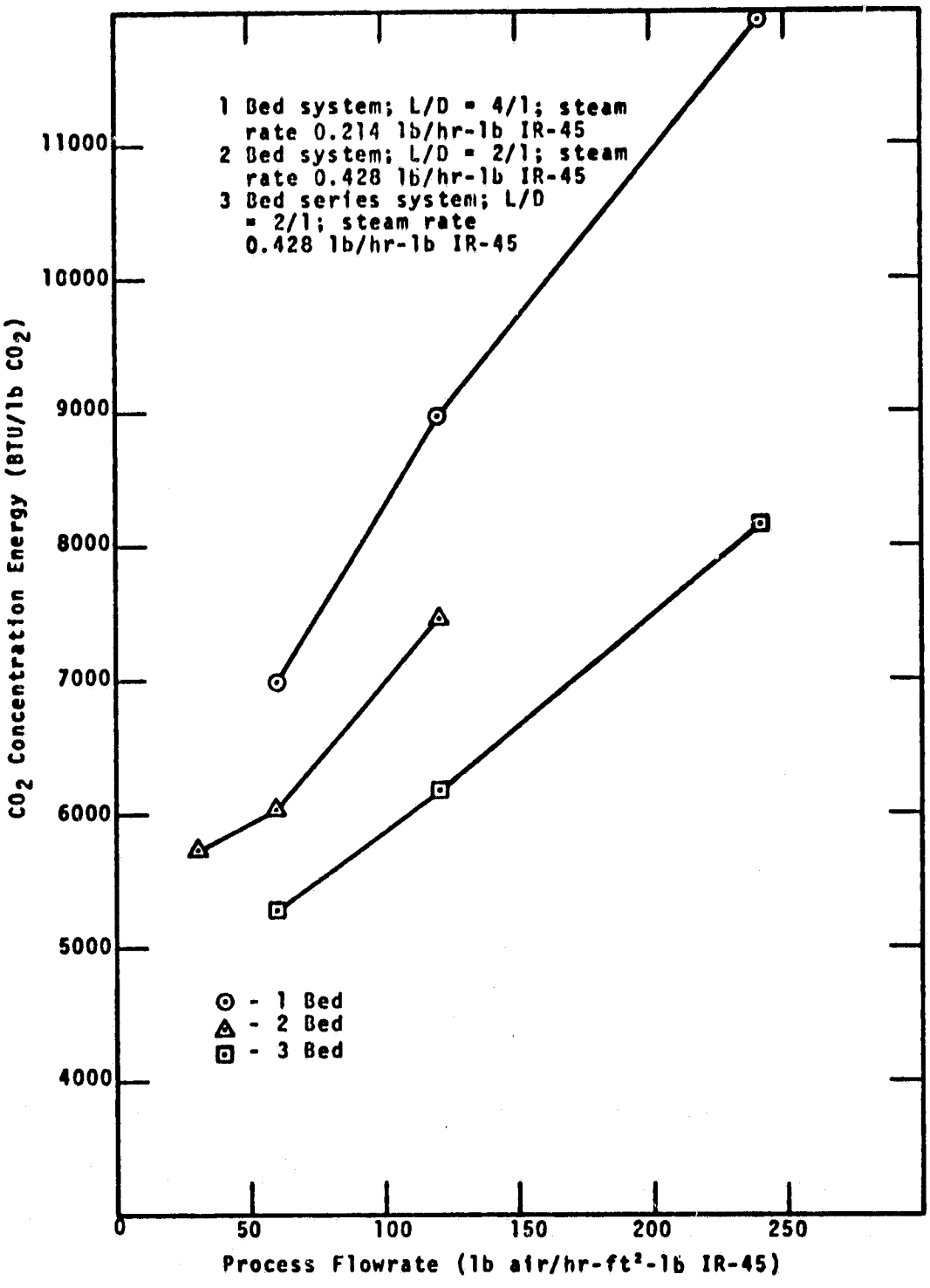

FIGURE 21 MULTI BED SYSTEM COMPARISON

For the 2-bed design, with each bed operating singularly, the three-way valves would be replaced with four-way valves controlled in the same manner as the 1-bed design. The 2-bed design also would require that the absorption and regeneration cycles be matched in time. This design, however, would enable the process fan to operate continuously thereby providing stable inlet process conditions and reduce the fan starting mode associated with the 1-bed design.

The 3-bed design with two beds operating in parallel or series would provide continuous operation. The 3-bed parallel operation may be considered a 2-bed system with a reduced process flowrate for each bed. The absorption cycle time for each bed would be twice the regeneration cycle time therefore requiring matching the cycle times similarly to the 2-bed design. The 3-bed series design would operate similarly to the 3-bed parallel design except that the process flowrate for each bed would not be reduced. Individual three-way valves both upstream and downstream of each bed would control the flow of steam or process flow to each bed. The required valves would add to system weight and complexity.

Heat Capacity of IR-45

An additional experiment was included to determine the heat capacity of IR-45. Heat capacity information was obtained by measuring the quantity of steam required to heat 1.612 lbs of IR-45 with 6% moisture content from 76 to 211°F. The IR-45 was contained by a 3.0 inch diameter glass bed 12 inches long. In the same manner, 6.62 lb of 0.25 inch Type 304 stainless steel raschig rings (reference C_p = 0.11 Btu/lb-°F) enabled estimating the heat loss to the surroundings. Equating the heat loss of the IR-45 and stainless steel tests allowed the heat capacity of the IR-45 to be derived.

Results.-Steam in the amount of 0.280 lb was required to heat the bed containing IR-45 from 76 to 211°F while the bed containing the stainless steel required 0.275 lb of steam to heat it from 65 to 211°F. The moisture content of the IR-45 after heating was determined by weight difference to be 20% indicating a 14% increase affected by the condensed steam.

Considering 211°F steam entering the stainless steel test, the total heat input was:

$$Q_{TSS} = m_{st}\lambda v = 0.275 \text{ lb} \times 971 \text{ Btu/lb}$$

$$Q_{TSS} = 267 \text{ Btu}$$

The heat required by 6.62 lb of stainless steel was:

$$Q_{SS} = mC_p\Delta T = 6.62 \text{ lb} \times .11 \text{ Btu/lb°F} \times (211-65)°F$$

$$Q_{SS} = 106 \text{ Btu}$$

The heat loss to the surroundings was:

$$Q_{Loss} = Q_{TSS} - Q_{SS} = 267-106 \text{ Btu}$$

$$Q_{Loss} = 161 \text{ Btu}$$

Total heat input to the IR-45 test was:

$$Q_{T\ IR-45} = m_{st}\lambda v = 0.280 \text{ lb} \times 971 \text{ Btu/lb}$$

$$Q_{T\ IR-45} = 272 \text{ Btu}$$

Equating the heat loss, the heat required by the IR-45 was:

$$Q_{IR-45} = Q_{T\ IR-45} - Q_{Loss} = 272-161 \text{ Btu}$$

$$Q_{IR-45} = 111 \text{ Btu}$$

Constructing a heat balance about the IR-45 with 20% moisture content, since this was the final condition:

$$Q = m_{IR-45}C_{pIR-45}\Delta T + \frac{m_{H_2O}}{m_{IR-45}}\ m_{IR-45}C_pH_2O\Delta T$$

$$111 \text{ Btu} = \left(1.518 \text{ lb} \times C_p \times 135°F + \frac{.249 \text{ lb}}{\text{lb}}\ 1.518 \text{ lb} \times 1 \times 135\right)\text{Btu}$$

$$\frac{(111-51)\text{Btu}}{205 \text{ lb } °F} = \frac{60 \text{ Btu}}{205 \text{ lb-°F}} = C_p$$

$$C_{pIR-45} = 0.29 \text{ Btu/lb°F}$$

Effect of IR-45 Moisture Content on CO_2 Capacity

Several experiments were performed to determine the influence of IR-45 moisture content on CO_2 capacity in the range of 5-20%. The >30 mesh particles were exposed to a process air stream of 72 ± 3°F temperature and 52 ± 2°F dewpoint, input CO_2 partial pressure 3.7 mm Hg and 0.5 CFM flowrate.

Results.-The IR-45 half-life CO_2 capacity was observed to increase from 0.011 lb CO_2/lb IR-45 at 5% moisture content to 0.024 lb CO_2/lb IR-45 at 20% moisture content. As the moisture content was increased from 10 to 12%, the half-life CO_2 capacity increased from 0.015 to 0.021 lb CO_2/lb IR-45 indicating that a minimum of 12% moisture content is required to provide greater than 0.02 lb

CO_2/lb IR-45 CO_2 capacity. Table 5 presents the half-life CO_2 capacity-moisture content data.

TABLE 5 - IR-45 MOISTURE CONTENT AND HALF-LIFE CO_2 CAPACITY

IR-45 Moisture Content (%)	Half-life CO_2 Capacity (lb CO_2/lb IR-45)
5	0.011
8	0.013
10	0.015
12	0.021
15	0.023
20	0.024

An absorption isotherm was derived in the previous investigation (NAS1-5277) and 100% humidity, 77°F process air resulted in 28% water load on IR-45. Thus, a water film is present on IR-45 for greater than 28% moisture content. Absorption tests performed with IR-45 containing greater than 28% moisture showed that the CO_2 capacity is degraded and that the moisture content of IR-45 should be maintained between 12 and 25% for optimal CO_2 absorption.

Boiler/Condenser Design for Zero-G Operation of CO_2 Removal System

Preliminary studies were conducted to determine the feasibility of using a hydroscopic salt such as lithium chloride to serve in a steam generator/steam condenser device designed for use in space, i.e., in the absence of gravity. These studies also included the evaluation of several materials to serve as support for the salt.

Experimental - Investigation of a support material. In order to avoid the caking which results when LiCl salt dissolves in water, a suitable support material is required. Such a material must hold the LiCl in a fixed position in the drying chamber during both air drying and steam generation phases of the proposed boiling/condensing operation. The following materials were considered and tested for applicability:

1. Carbon granules - large surface area
2. Chamois cloth - natural hide

3. Bentonite clay - aluminum silicates with traces of Mg and Fe

4. Perlite - a glassy rock material consisting of:

65-75% SiO_2
10-20% Al_2O_3
2-5% H_2O

5. Vermiculite - a light-weight, high surface area material consisting of:

34% SiO_2
21% MgO
15% Al_2O_3
9% Fe_2O_3
5-7% K_2O
1% CaO
5-9% H_2O

and traces of Cr, Mn, P, Si and Cl. Most of the tests involved this support material.

Steam condensation and absorption. - The experimental apparatus consisted of 18 inch long glass tubes with cooling jackets, boiler, infrared water vapor monitors and preformed Teflon tubing. The screen sized vermiculite particles were loaded with LiCl by adding a nearly saturated solution of LiCl in H_2O to an evacuated (2 mm Hg) flask containing the vermiculite. The bed was then baked to remove water. In one series of tests, 36 gm of vermiculite are loaded with 36 gm of LiCl by first dissolving the salt in 60 ml distilled H_2O; then oven-drying the soaked vermiculite to an equilibrium weight of 74.6 gm which includes a water content of about 5% of the combined vermiculite/salt weight. Since the solubility of LiCl in water (at 20°C) is 0.8 gm/gm H_2O, the prepared LiCl-vermiculite bed should absorb a maximum of 45 gm of H_2O.

The steam condensing capacity of the LiCl/vermiculite column was tested by transferring steam from a freshly regenerated IR-45 bed. The size of the IR-45 bed and the flowrate of the air used to transfer steam were scaled to correspond to the size of the LiCl-vermiculite drying column, a 200 gm (dry wt) resin bed with a 1/1 L/D ratio was used. Based on a heat capacity of 0.29 Btu/lb-°F, such a bed requires 8 gm of steam for regeneration. The air flow rate used to transfer the steam was 3.75 CFH. The effective crossection of the drying column was 0.9 in^2, this flowrate corresponds to a 25 CFM flow through a 14 inch diameter resin bed.

The water removal efficiency of the drying column was measured by passing a portion of the effluent air through a LIRA infrared analyzer.

Results.-

1. Carbon - Considerable migration of the LiCl occurred when the salt-loaded carbon granules were used in a simple bed. This problem was reduced by placing the loaded granules between the walls of concentric cylinders.

2. Chamois cloth - Provided a good support for LiCl but became distorted, hard and brittle upon drying or heating.

3. Bentonite clay
4. Perlite

These materials caked when moist

5. Vermiculite - This material supported 200% of its own weight of LiCl. Some migration of salt did occur, however this effect was minimized by screening the vermiculite so that the mean thickness of each particle used measured approximately one tenth of the bed diameter.

A drying column consisting of LiCl deposited on vermiculite indicated possible feasibility as a boiler/condenser. Additional work is required, however, to evolve an acceptable prototype unit.

Although a 2/1 weight ratio of LiCl to vermiculite is obtainable such loading usually resulted in gross migration of the LiCl through the bed. A 1/1 ratio resulted in very little salt migration.

The lithium chloride vermiculite combination provided effective drying of moist air. Drying action was considerably improved when the LiCl/vermiculite bed was maintained at ambient temperature during the condensation period. The linear velocity of steam passing through the drying column must be sufficiently low to prevent migration of the LiCl. This problem may be alleviated by passing steam alternately in both directions through the bed.

Results of drying tests conducted with an uncooled dryer are shown in Figure 22, curve A. The average amount of water collected during a 27 minute drying test was about 15 gm.

The solubility of LiCl in water ranges from 0.8 gm/gm H_2O at 20°C to 1.30 gm/gm H_2O at 95°C. In order to take advantage of the increased water capacity at lower temperatures a coolant filled jacket was fitted around the drying column. Drying tests were then conducted as before with the dryer maintained at 65°F. Results are shown in Figure 22, curve B. The average amount of water collected increased to 19 gm.

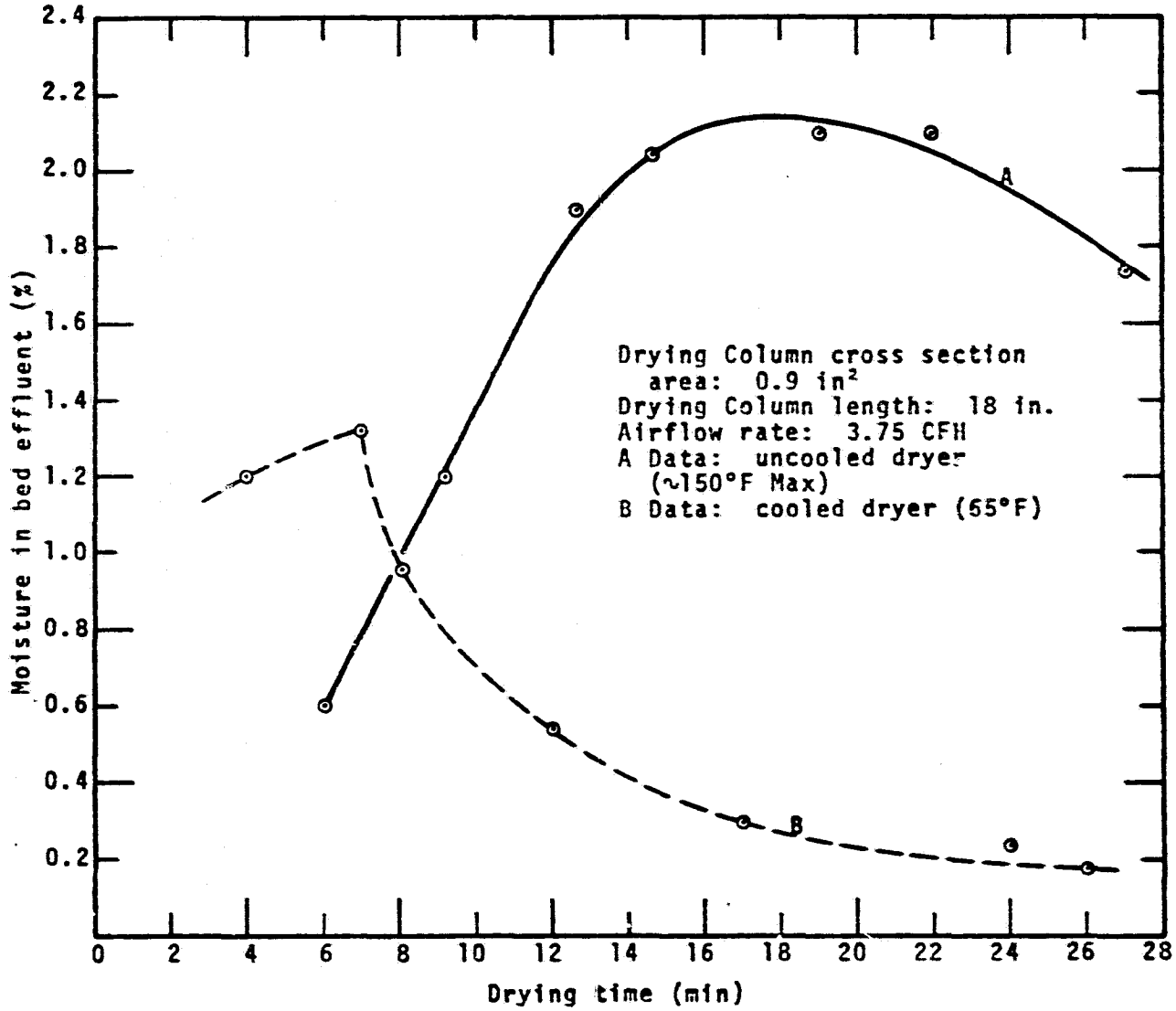

FIGURE 22 DRYING CURVES FOR LiCl-VERMICULITE

The ability of the drying column to function as a steam generator was then tested by heating the column used in the tests discussed above. Temperatures in excess of 325°F were required to raise the vapor pressure sufficiently to produce steam. Further testing showed that when the drying column is loaded to about 80% of its capacity adequate vapor pressure to produce steam may be achieved between 275 and 300°F. However, when the drying column is wetted beyond 50% capacity the LiCl tends to migrate from one vermiculite particle to another and to the walls of the column.

Analysis of Task I Data

Factorial analysis was applied to the results of experiments conducted to determine the influence of particle size, process flowrate, bed L/D and IR-45 moisture content on IR-45 CO_2 capacity. The process flowrate and bed L/D were combined as residence time which was then used with particle size and moisture content in a factorial analysis. Table 6 presents the parameter level used for analysis.

TABLE 6 - PARAMETER LEVEL FOR FACTORIAL ANALYSIS

Parameter level	+	-
Particle size (mesh)	<40	>30
Residence time (sec)	6.0	1.5
Moisture content (%)	20	6

The IR-45 CO_2 capacity determined for the bed half-life was used in the analysis. Table 7 presents the factorial experiments and CO_2 capacity where the particle size, residence time and moisture content are X_1, X_2 and X_3 respectively.

TABLE 7 - FACTORIAL EXPERIMENT LEVELS

Particle size (X_1)	Residence Time (X_2)	Moisture Content (X_3)	CO_2 Capacity (%) C
-	-	-	0.72
+	-	-	0.41
-	+	-	1.07
+	+	-	1.15
-	-	+	2.20
+	-	+	1.98
-	+	+	2.20
+	+	+	2.20

A replicate of Table 7 experiments was performed. The resultant dependence of CO_2 capacity on the parameters was expressed as:

$$C = 1.500 - 0.006X_1 + 0.178X_2 + 0.666X_3 + 0.084X_1X_2 + 0.011X_1X_3 + 0.051X_2X_3 + 0.057X_1X_2X_3$$

Subsequently, the particle size parameter was deleted from the analysis and only the residence time and moisture content effects were included. The CO_2 capacity was then expressed as:

$$C = 1.547 + 0.087X_2 + 0.652X_3 + 0.087X_2X_3$$

TASK II PROCESS MODEL DEVELOPMENT

A 4-man size test system was assembled as described by Figure 23 to obtain data from which an operational model of the CO_2 concentration process could be derived. The system was enclosed in a 120 cu ft chamber into which CO_2 was injected to maintain a 3.8 mm Hg CO_2 partial pressure. A fan (Rotron Model SL4A2FM) was used to circulate the process air through the absorption system which included: a heat exchanger which controlled the inlet air temperature to the sorber bed, a flow meter (Vol-o-Flo Model 50-1-30), calibrated for air, the sorber bed and process condenser. During regeneration, steam was injected into the sorber bed which was isolated from the absorption system by associated valving. The sorber bed void air and CO_2 passed from the sorber bed, out of the 120 cu ft chamber, through a condenser, flow meter (Vol-o-Flo Model 50-1-3) calibrated for CO_2, sampling manifold and dry test meter.

The sorber bed used for the majority of tests was 15.9 in. ID x 8 in. long closed at the ends by 16 in. radius dished heads. The IR-45 was supported at the inlet and outlet by "Nevaclog" plates. Temperatures were monitored with thermocouples located at the fan outlet, process air flowmeter inlet, sorber bed inlet, 2 and 6 in. into the IR-45, sorber bed outlet, condenser inlet and outlet and the inlet to the regeneration condenser. Resistance probes for monitoring the IR-45 moisture content were located at 2 and 6 in. into the IR-45.

The CO_2 input to the chamber was regulated by a CO_2 LIRA (MSA Model 300) controller combination which opened a solenoid valve when the LIRA indicated that the chamber CO_2 partial pressure became less than 3.8 mm Hg. Total CO_2 input was determined by CO_2 bottle weight difference. The system outlet CO_2 concentration was monitored downstream of the process condenser with another CO_2 LIRA (MSA Model 300). The steam flowrate was valve regulated and the actual rate determined by observing the weight of water supplied to the steam generator with time. The system moisture balance was determined by comparing the quantity of steam supplied with the sum of the process and regeneration condensate.

The process flowrate was regulated with a control valve downstream of the process condenser. The system inlet and outlet air dewpoints were monitored with moisture LIRAs (MSA Model 300).

Results

Analysis of the Task I data showed that maintaining the IR-45 moisture content balance is the most important parameter influenc-

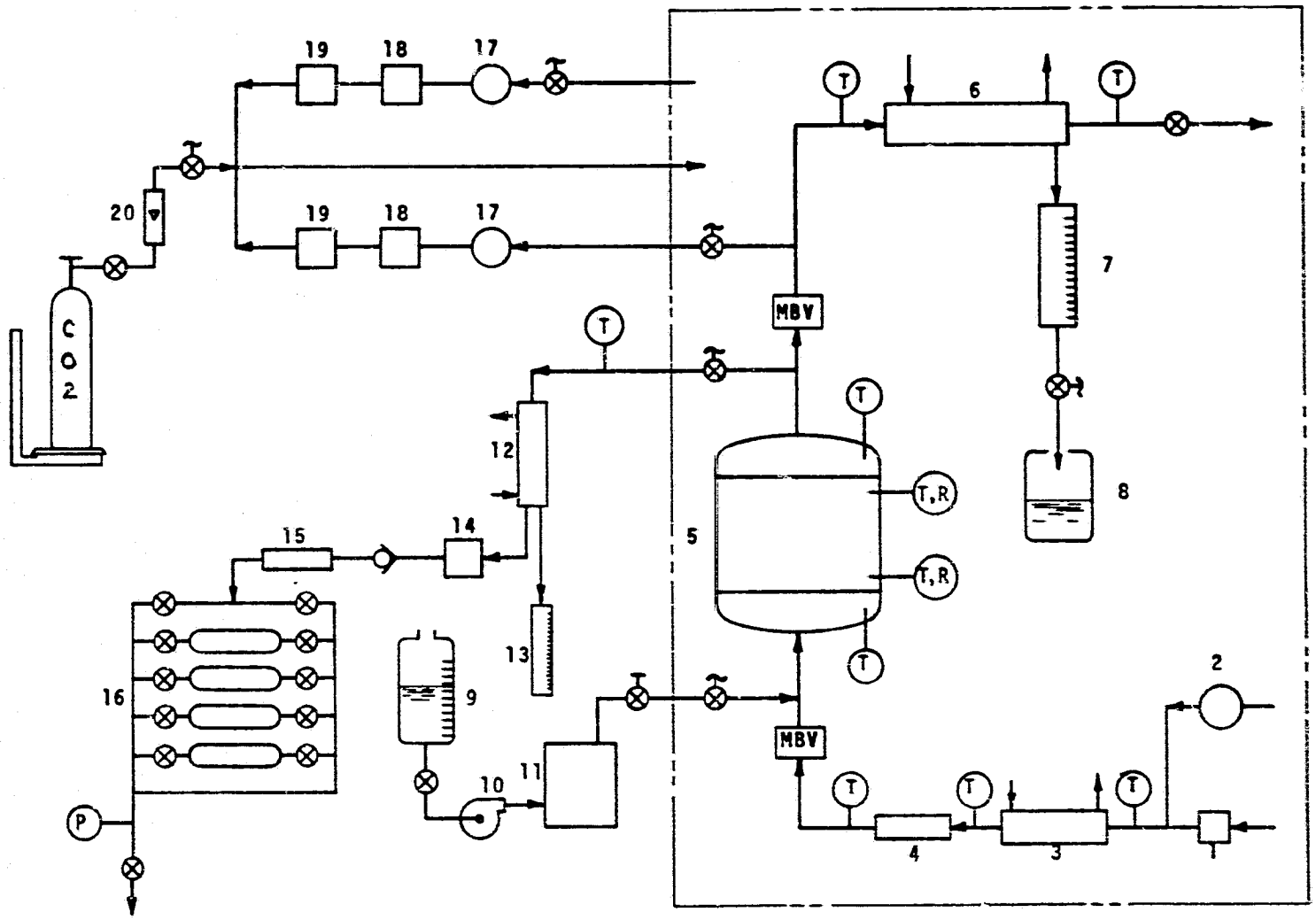

FIGURE 23 TASK II TEST SYSTEM

1 Fan

2 ΔP Transducer

3 Heat Exchanger

4 Flowmeter

5 Sorber bed

6 Condenser

7 Condensate Collector

8 Condensate Reservoir

9 Water Reservoir

10 Water pump

11 Boiler

12 Condenser

13 Condensate Collector

14 O_2 Monitor

15 CO_2 flowmeter

16 Sampling Manifold

17 Pump

18 CO_2 LIRA

19 H_2O LIRA

20 CO_2, Scale, Flowmeter

MBV Motor-operated Ball Valve

⊗ Solenoid Valve

⊗ Valve

Ⓟ Pressure Guage

Ⓣ Temperature

Ⓣ,Ⓡ Temperature, Resistance

ing the system CO_2 capacity and energy requirements. Process air flow and bed length to diameter were related in Task I to residence time. IR-45 CO_2 dynamic capacity at bed half-life was shown to be inversely related to the residence time. Although the Task I data were obtained with quasi-steady state conditions, a similar effect of residence time on CO_2 capacity is expected with transient conditions if the IR-45 moisture content balance can be maintained.

Maintaining the IR-45 moisture content balance requires that process conditions exist such that the quantity of steam added to the sorber bed during regeneration is removed during absorption. If insufficient or excess moisture is removed, the IR-45 will either become too wet or dry for optimal CO_2 capacity. A mass and heat balance for the process air and IR-45 must be obtained to assure the IR-45 moisture content.

A series of tests were conducted to determine the performance of IR-45 as a function of absorption time, process air flowrate, air temperature and humidity. The test conditions are presented by Table 8 . Since the character of the IR-45 moisture content balance may not be degraded through a few cycles of operation, those tests which did not immediately cause a moisture content unbalance were run for a maximum of 100 hours. These data, however, do not lend itself to common linear analytical models or can they be presumed steady state even after 100 hours; therefore, factorial type models also are not strictly reliable. The model approach used for representing the moisture balance process was based on the heat and mass transfer occurring during absorption. Six series of tests were performed and those test results used for model derivation are presented by Table 9 .

Mathematical Model.-The mathematical model is a set of differential equations expressing the heat and mass balance and heat and mass transfer affected by the process air, IR-45 and moisture system. These were converted to finite difference form.

The water evaporating from the IR-45 bed is given by

$$\text{delW} = K(18.0)\ln \frac{p-prw}{p-paw} \qquad \text{(eq. 1)}$$

where del W = mass flowrate ($lb/min\text{-}ft^3$)
K = mass transfer coefficient ($Moles/min\text{-}ft^3$)
p = pressure (psi)
prw = water vapor saturated pressure (psi)
paw = water vapor partial pressure (psi)

The log term is chosen from theoretical grounds. The amount of water evaporating is proportional to the log mean of the inert process gas pressure and the difference in water vapor partial pressure at the bed.

TABLE 8 - TASK II TEST CONDITIONS

Ab. time (min)	Flowrate (CFM)	Air temperature (F°)	Air dewpoint (°F)
60	15	120	60
60	30	120	60
30	15	120	60
30	30	120	60
60	15	120	85
60	30	120	85
30	15	120	85
30	30	120	85
60	15	70	45
30	30	70	45
30	15	70	45
60	30	70	45
60	15	70	65
60	30	70	65
30	30	70	65
30	15	70	65

TABLE 9 - ABSORPTION TEST RESULTS

Test No. A5
Process Flowrate: 29.8 CFM
Chamber dewpoint: 54 ± 3°F
System Pressure: 40 in. H_2O

Absorption time (min)	Inlet temp. (°F)	Inlet plenum temp. (°F)	Bed temp. (°F) in	Bed temp. (°F) out	Exit air temp. (°F)	Cumulative condensate (lb water)
3	105		155	175	182	1.65
5	111		112	148	163	1.87
8	112		92	125	146	2.09
10	113		84	115	136	2.26
15	117		77	98	111	2.46
20	121		75	92	98	2.60
25	122		74	91	86	2.72
30	122		74	90	83	2.80

Test No. D5
Process Flowrate: 25.8 CFM
Chamber dewpoint: 49 ± 3°F
System Pressure Drop: 44 in. H_2O

3.3	116	110	140	160	166	1.76
6.7	118	106	112	137	159	2.46
10.0	121	105	97	123	137	--
16.7	123	102	87	105	121	--
20.0	123	102	86	99	115	3.54
30.0	125	104	84	90	102	3.85
40.0	126	105	84	87	94	4.00
50.0	126	107	85	87	88	4.14
60.0	126	110	85	86	86	4.20

TABLE 9 (continued)

Test No. D41
Process Flowrate: 28.5 CFM
Chamber dewpoint: 50 ± 3°F
System Pressure: 41 in. H_2O

Absorption time (min)	Inlet temp. (°F)	Inlet plenum temp. (°F)	Bed temp. (°F) in	Bed temp. (°F) out	Exit air temp. (°F)	Cumulative condensate (lb water)
3	82	113	114	138	167	--
6	87	112	91	112	151	2.75
10	87	100	85	94	130	3.17
16	85	91	80	88	113	3.70
26	84	85	75	79	86	4.05
37	84	82	72	75	85	4.21
49	84	82	72	74	79	--
57	84	82	72	74	77	4.33
60	84	82	72	74	76	4.40

Test No. E37 and 43
Process Flowrate: 31.3 CFM
Chamber dewpoint: 58 ± 3°F
System Pressure Drop: 40 in. H_2O

3.3	122	117	140	165	165	1.54
6.7	125	117	100	128	141	1.98
10.0	127	115	89	111	128	2.20
13.3	130	115	85	103	117	--
16.7	130	116	83	99	111	--
20.0	131	116	81	98	106	--
30.0	134	119	80	95	95	3.04
3.3	121	113	134	158	165	1.34
6.7	124	113	93	121	134	--

TABLE 9 (continued)

Absorption time (min)	Inlet temp. (°F)	Inlet plenum temp. (°F)	Bed temp. (°F) in	Bed temp. (°F) out	Exit air temp. (°F)	Cumulative condensate (lb water)
10.0	126	113	87	104	118	2.16
13.3	128	114	84	98	111	--
16.7	129	115	82	95	105	--
20.0	131	116	80	92	99	--
30.0	133	117	78	88	89	3.06
Test No. E45 and 51						
Process Flowrate: 15.7 CFM						
Chamber dewpoint: 62 ± 3°F						
System Pressure: 51 in. H_2O						
3.3	121	127	138	165	160	--
6.7	123	119	105	141	144	2.26
10.0	123	115	92	124	132	--
16.7	125	111	88	112	123	2.31
20.0	128	110	82	98	108	--
26.7	131	110	79	93	100	2.84
33.3	132	110	77	91	95	--
40.0	133	112	76	88	91	3.03
50.0	135	114	75	86	89	3.16
60.0	135	114	75	85	86	3.30
3.3	118	129	145	167	168	--
6.7	120	120	108	145	148	2.02
10.0	122	113	96	122	134	2.24
13.3	123	110	91	111	126	--
20.0	127	109	86	98	109	2.64
26.7	129	109	84	96	104	2.79
33.3	131	110	82	92	99	2.92
40.0	133	111	82	92	96	3.05
50.0	134	112	81	91	93	3.21
60.0	134	114	80	90	91	3.30

The water content of the bed is

$$\frac{\partial W}{\partial \Theta} = \frac{delW}{\rho} \qquad \text{(eq. 2)}$$

where W = IR-45 moisture content (lb/lb)
Θ = time (min)
ρ = IR-45 density (lb/ft³)

The heat transfer is

$$delQ = h(T_{air}-T_{bed}) \qquad \text{(eq. 3)}$$

where delQ = heat flow (Btu/min-ft³)
h = heat transfer coefficient (Btu/min-ft³)
T = temperature (°F)

The heat balance for the bed is

$$\frac{\partial T_{bed}}{\partial \Theta} = \frac{(delQ + \lambda delW)}{(C_{pb} + (C_{pw})(W)\rho} \qquad \text{(eq. 4)}$$

where λ = Latent heat of vaporization (Btu/lb)
C_{pb} = heat capacity of IR-45 (Btu/lb-°F)
C_{pw} = heat capacity of water (Btu/lb-°F)

The mass balance for the steam is

$$\frac{\partial V}{\partial \ell} = \frac{-delW}{18} \qquad \text{(eq. 5)}$$

where V = Molar velocity (Moles/min-ft²)
ℓ = length (ft)

The mass balance for the steam in the air is

$$\frac{\partial(Vpaw/p)}{\partial \ell} = \frac{-delW}{18.0} \qquad \text{(eq. 6)}$$

The heat balance for air is

$$\frac{\partial(TairVCp)}{\partial \ell} = -\frac{delQ+delW\ T_{bed}Cps}{18} \qquad \text{(eq. 7)}$$

where $Cp = Cpa + \frac{paw}{p}(Cps-Cpa)$
Cpa = heat capacity of air (Btu/mole-°F)
Cps = heat capacity of steam (Btu/mole-°F) (eq. 8)

In general, the above equations were used for all the models. Various models were tested. One model changed equation 1 to

$$delW = K'18\ (paw-prw) \qquad \text{(eq. 9)}$$

This gave no better fit and indeed seemed to fit less well.

In another model, euqations 1 through 8 were slightly altered to account for a screening effect as the water vapor diffuses outward from the bed particles. Again no great effect was noted.

Since h and K can be expected to vary with vapor velocity, equations 1 and 3 were changed to

$$delW = K''18\ V^{0.5} \ln \frac{p-prw}{p-paw} \qquad \text{(eq. 10)}$$

$$delQ = h\ V^{0.5}(T_{air}-T_{bed}) \qquad \text{(eq. 11)}$$

The analysis of the previous models had been hampered by the fact that the adiabatic humidification line implied by the data was not parallel to the conventional adiabatic humidification line of a wet bulb chart. This further implies a heat source during humidification. The latest model, in effect, includes this heat source by making a fog correction.

An analogy is a body of warm water such as a lake in contact with cold air. The water evaporates, and the hot influent vapor heats the bed void air. However, if the air is sufficiently cold, the resultant air vapor temperature may cause condensation and fog formation in the bed.

In the earlier set of equations, there is nothing to prevent the partial pressure of water (paw) from becoming greater than the vapor pressure of water at the air temperature, T_{air}. In the updated model the vapor pressure is limited to saturation pressure.

If the air would be supersaturated by the use of equations 1 through 11, a portion (0.1%) of the water vapor in the air is condensed. The water vapor partial pressure is reduced, and the latent heat of condensation heats the air. If the air at the new temperature and partial pressure is still supersaturated, the process is repeated. The condensed water is then considered to reabsorb on the bed. This then gives a mechanism to add heat to the air

The optimum h and K values have not been found, but the h and K values found by preliminary search give the best data fit to date.

Analysis of the Models.-The various models were tested by comparing predicted bed and air temperatures versus time results with experimental data. The process is essentially a three step process.

1. Select candidate h and K values, and run the model.

2. Repeat step 1 until h and K have been selected such that the residuals (actual temperatures - predicted temperature) have been reduced to a minimum.

3. For the optimum h and K, examine the residuals and compare the various models.

Figure 24 presents a flow chart of the computer program used to evaluate the various models. The latest form of the computer program is presented on pages 78 and 79.

The optimization of h and K is difficult and time consuming because the model is highly nonlinear and the search is nonlinear. The minimum residual will usually be reached only after several trials and even then the optimal h and K values may not be obtained.

The first model tested consisted of equations 1 through 8. Three criteria for optimization were used.

1. the sum squares of error for the bed entry temperatures

2. the sum squares of error for the bed exit temperatures

3. the sum squares of error for the exit air temperatures.

Unfortunately, the h and K optimums were not the same for the three criteria. Table 10 gives the results. When h, K were optimized for one criteria, the sum square error for the others would increase by 50%.

One other criticism of the fit is that the residuals indicated a trend with time. At early absorption times, the predicted temperatures were higher than the experimental temperatures, and at late absorption times, the behavior reversed.

Model II, consisting of equations 2 to 9, behaved similarly to Model I. The average error for Model II was less, but the optimum h and K values for these criteria were even wider spread.

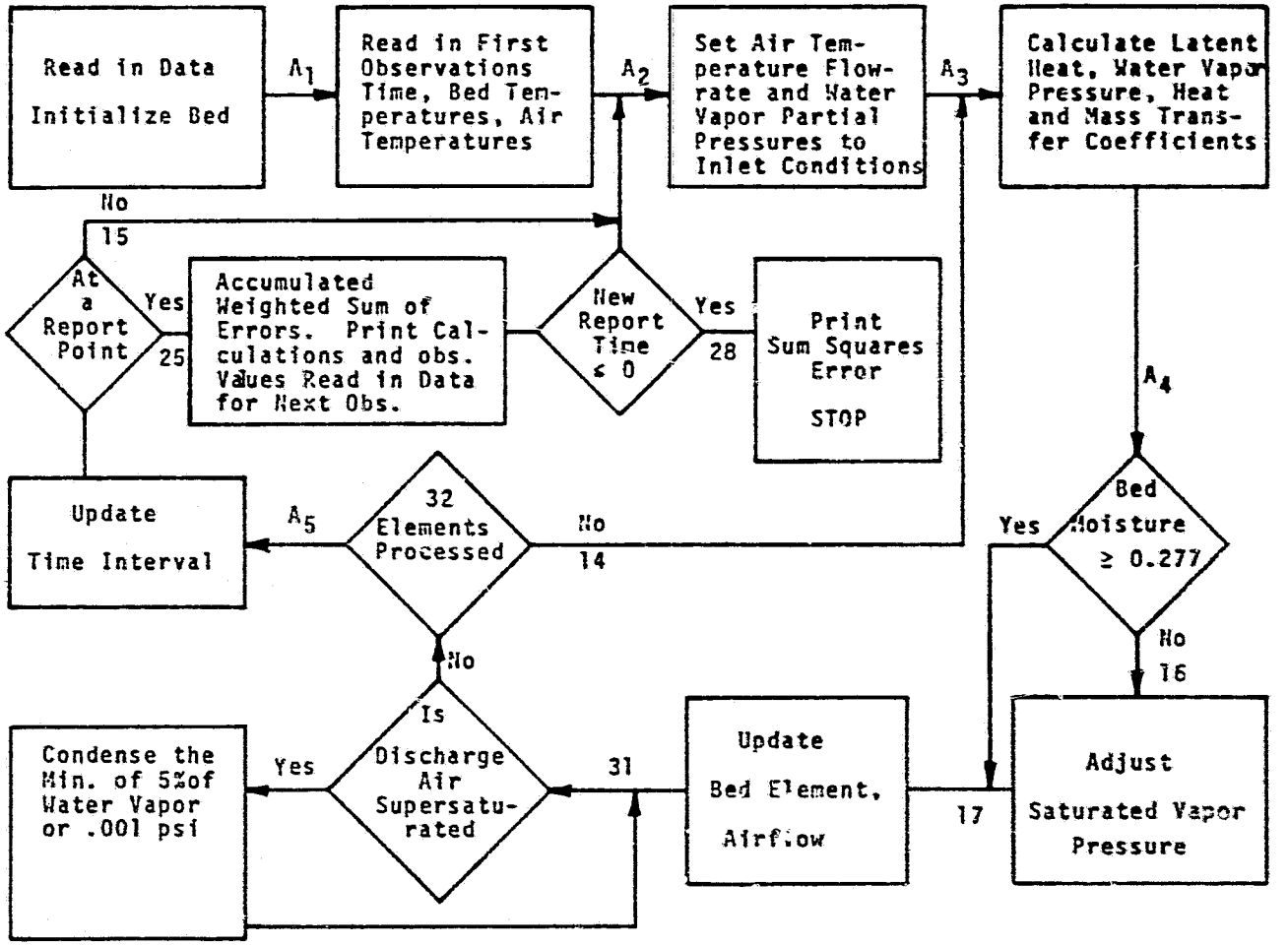

FIGURE 24 COMPUTER MODEL FLOW CHART

TABLE 10 - MODEL I RESULTS

Data	h	K	Avg. Error	Criteria
A5	500	2	20.3°F	bed entry
A5	500	1.5	7.76°F	bed exit
A5	500	1.0	10.95°F	exit air
E37	15	3.0	5.9°F	bed entry
E37	300	1.5	5.56°F	bed exit
E37	300	1.0	1.39°F	exit air
E51	30	3.0	4.97°F	bed entry
E51	80	1.35	5.15°F	bed exit
E51	68	0.9	1.76°F	exit air

TABLE 11 - MODEL II RESULTS

Data	h	K	Avg. Error	Criteria
A5	8	0.15	9.4°F	bed entry
A5	250	0.12	6.21°F	bed exit
A5	500	0.1	7.7°F	exit air temperature.

In an effort to obtain a better fit and a more complete understanding of the system, attention was focused on the quasi-steady state which would be obtained near the end of the absorption. After a bed has run for a sufficiently long time, and provided the bed does not dry out, the bed will have a constant equilibrium temperature, and the air will have a characteristic temperature pattern. The coefficients h and K were selected to minimize the sum square errors between predicted and actual bed entry temperatures, bed exit temperature, and exit air temperature. The error is taken to be

$$\xi^2 = W_1(T^p_{Ben} - T^a_{Ben})^2 + W_2(T^p_{Bex} - T^a_{Bex})^2 \qquad \text{(eq. 12)}$$

$$+ W_3(T^p_{exit} - T^a_{exit})^2$$

where the W_1, W_2 and W_3 are weighting coefficients and the super scripts refer to predicted and actual temperatures.

The bed and exit air temperatures used were the last data points measured; the 30 minute data for test E37 and 60 minute data for tests E51, D5 and D41.

Because of the extensive trials required, a pattern search was set up to automatically converge to the optimum.

Table 12 gives the optimum h and K and the average error for these runs. The weighting constants used in equation 12 were 0.25, 0.25 and 0.5. This gives equal weight to the exit air temperature and the bed temperatures. The two internal bed temperatures are given equal weight.

The runs were made using two different inlet temperatures, one temperature being the process flowmeter inlet temperature and the other being the inlet plenum temperature.

These h and K values were still not satisfactory for two reasons: the experimental data for both E37 and E51 showed the bed exit temperature greater than the bed entry temperature, while the model predicts the reverse. Also, the h and K values should be smoothly related to the molar flowrate. However, a plot of Log h or Log K versus Log flowrate had large scatter.

TABLE 12 - QUASI-STEADY STATE RESULTS

Data	Inlet Temp. (°F)	h	K	Square Root of error^2(°F)
E37	119	0.7	0.0363	6.55
E37	134	0.89	0.08135	6.4
E51	114	0.404	0.0254	4.5
E51	134	0.5866	0.08962	3.73
D5	110	1.03	0.02575	5.9
D5	126	1.13	0.0565	6.78
D41	82	0.5343	0.01264	1.73
D41	84	0.6495	0.01779	2.09

The increase in bed temperature with distance is contrary to the adiabatic humidification curve. For the air-water system, the adiabatic humidification line and the wet bulb line are identical. This means that the wet bulb temperature should be constant throughout the bed.

Indeed, since mass transfer can be decreased relative to heat transfer (by partial drying of the resin surface while maintaining water deep in the particle), one could postulate a decrease in bed temperature with distance.

The increase of bed temperature with distance implies that there is a heat source in the bed. However, because of the porous nature of the bed, heat transfer is small, and it is difficult to get a heat flow large enough to effect the drying curve.

Carbon dioxide is being absorbed by the bed and there is a heat of reaction. However, since the CO_2 content of the air is small, this heat source is small (5 Kcal/mole).

The temperature of the bed near the discharge, the "bed exit temperature", was also hotter than the adiabatic humidification curve would suggest. This would imply a source of heat or inlet air conditions (temperature or humidity) radically different. The temperature is considered correct because otherwise the inlet temperature would have to be much, much hotter than actual measurements. For example, 95°F wet bulb with 56°F dewpoint air would mean an inlet temperature of 210°F. The change in the inlet humidity would also be large (0.2 psia to 0.8 psia) but there may be a possible explanation of this. The air in the test chamber has a 56°F dewpoint humidity, and this will normally be the humidity entering the bed. However, there is a chance that liquid water would leak from the bed, enter the air heat exchanger and raise the air humidity.

However, the model showed no particular preference for the higher moisture content. The search for h, K and humidity was not carried to the full optimum but the optimum seemed to be in the direction of previous h and K values and the low humidity inlet.

The model was then changed to allow h and K to vary with flowrates, thereby giving a high h and K during the early drying period and a lowe value later. Again a full search was not employed, but results did not indicate a sufficient convergent effect.

At this time further attention was given to the model. As originally constructed, there was no constraint on the saturation of the air. Water diffuses into the air, proportional to the partial pressure difference. Heat diffuses into the air, proportional to the temperature difference. Both of these processes will give fully saturated air after sufficient time and bed depth. However, application of the original equations could lead to supersaturated air.

In nature, when this occurs, the water condenses as a fog and gives up its latent heat of vaporization. Consider a warm

body of water in contact with cold air. Because of the partial pressure gradient, water must evaporate. Simultaneously, the air is heated because of the temperature gradient. However, if the water transfer is large enough, more water will be transferred than the air can hold. The water condenses and the fog forms.

The mathematical model was altered to prevent supersaturation. Water transfer proceeds by a 2 step process. In step 1, moisture is added to the air by the set of equations previously used. Then the air is checked for supersaturation. If the air is supersaturated, sufficient water is condensed to make the air not supersaturated. The condensation relieves supersaturation by heating the air and by decreasing the water vapor partial pressure. The water condensed is returned to the bed at air temperature, giving an additional cooling action.

The E37 data was run against this last model using h and K values proportional to the square root of the molar flowrate. For h = 2.0, K = 0.132, with weighting factors 0.25, 0.25 and 0.5, the average error is 12.7°F.

The fog model does predict a rising bed temperature with bed depth, similar to experimental results. For h = 1.56 and K = 0.158, the predicted bed temperature difference between the entry and exit levels is 1.7°F versus the experimental 15°F, measured at the 30 minute point. The average error is 11.9°F. Figure 25 presents a comparison of the fog model predictions and experimental data.

The comparison trend of predicted and measured temperatures was similar for tests performed with the different process conditions. The measured temperature of the lower bed was approximately 20°F less than the predicted temperature while the upper bed and exit air temperature comparison provided a better correlation.

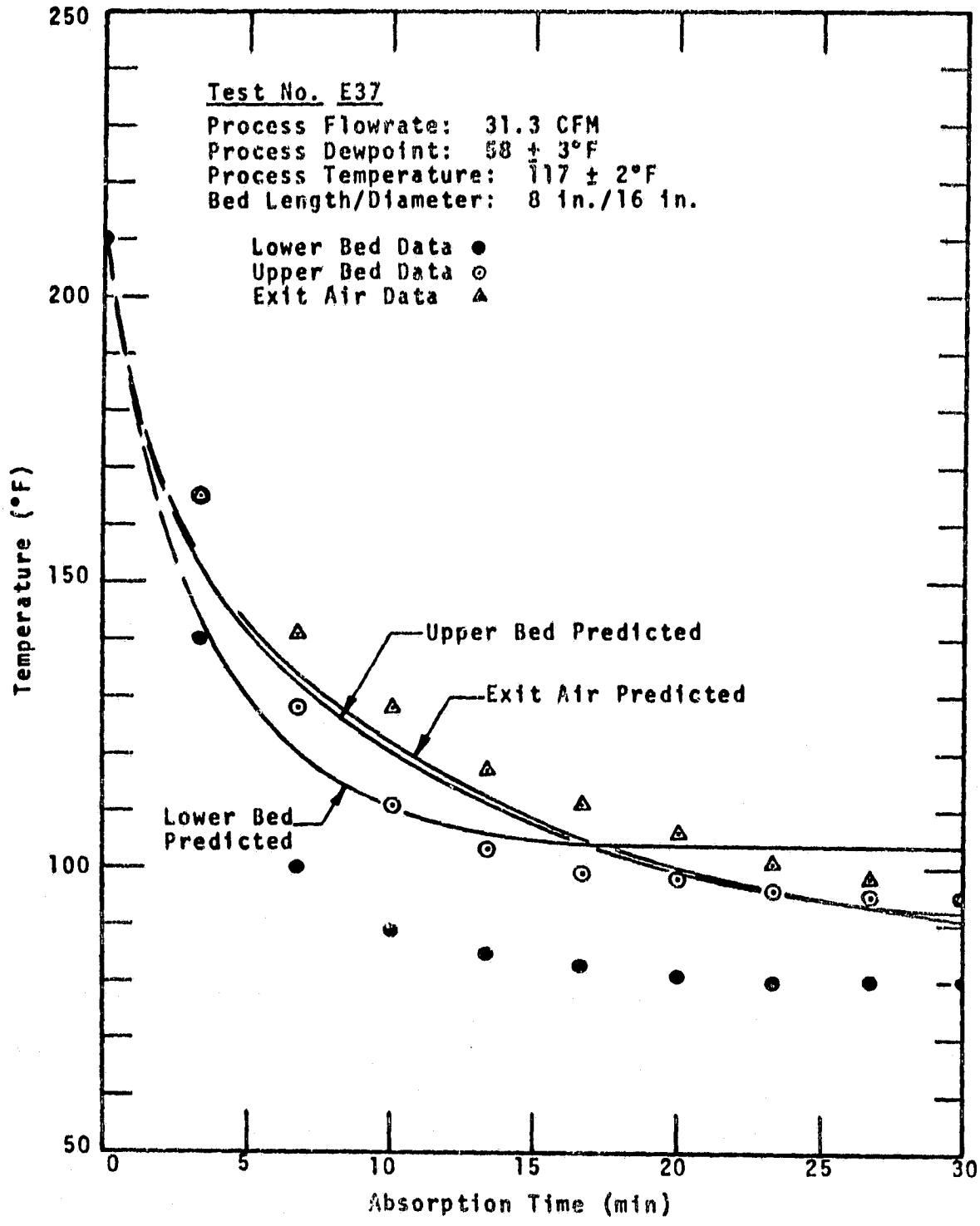

FIGURE 25 IR-45 BED TEMPERATURE HISTORY

TASK IV SORBER IMPROVEMENT INVESTIGATION

Upon evaluation of the IR-45 characteristics and requirements, two operational features were determined to effect, primarily, the use of IR-45 for CO_2 removal and concentration. These features are:

1. Maintaining proper IR-45 moisture content
2. Thermal requirement for regenerating IR-45.

The use of IR-45 for CO_2 removal and concentration is strongly constrained by the IR-45 moisture content being maintained and balanced through continuous absorption-regeneration cycling. Excessively drying the IR-45 will decrease its CO_2 removal capability. A continual increase of moisture content to approximately 28% when free water is present will also decrease CO_2 removal capability. Deterioration of the moisture balance, either too dry or wet, out of the optimal range (15-24%) also will change the sorber heat capacity and effect the time cycle for regeneration.

The quantity of steam required for regenerating IR-45 was determined in Task 1.5 and includes the heat capacity of zero moisture content IR-45 which was determined to be 0.29 Btu/lb-°F. A sorber with less heat capacity would reduce the thermal requirement for regeneration and reflect a lower power requirement. With these factors dominating, studies were performed to provide an improved sorber.

Some in-house work[3] indicated that several amines were promising candidates for an advanced CO_2 sorber. Impregnating a substrate material of lower heat capacity, than the styrene divinylbenze copolymer (IR-45), such as carbon (0.18 Btu/lb-°F) would be favorable. Pittsburgh activated charcoal Type BPL, impregnated with piperazine to 23 wt % was selected for this study. CO_2 sorption characteristics included in this study were:

1. Moisture content
2. Cycling effects on CO_2 capacity
3. Flowrate effects on CO_2 capacity
4. CO_2 equilibrium capacity

The sorber was prepared by dissolving 30 gm piperazine in 50 cc of water and impregnating 50.8 gm of dry 12x30 mesh BPL charcoal. The quantity of solution was just sufficient to wet the charcoal and filtration was not required. After thoroughly mixing, the charcoal was air dried for 20 hours and then vacuum dried at 65°C for 3 hours. The charcoal had a total weight of 66 gm of which 15.2 gm was considered to be piperazine.

Results.-The sorption studies were performed with 50 gm quantities of sorber contained in a 1.2 in. ID glass tube. The sorber was subjected to 20 cycles of sorption-steam regeneration to determine the effect of cyclic operation on CO_2 capacity. These cyclic studies were performed with 3.7 mm Hg CO_2 partial pressure, 5 lpm process flowrate at 75°F and 55°F dewpoint and a 9% sorber moisture content. The sorber CO_2 concentration for initial effluent CO_2 detection was 0.013 lb CO_2/lb sorber and the saturation concentration 0.033 lb CO_2/lb sorber. Both of these capacity values gradually decreased however and after 20 cycles were 0.010 lb CO_2/lb sorber and 0.018 lb CO_2/lb sorber, respectively. The adsorption curves for several cycles are shown by Figure 26 The change of breakpoint concentration with cyclic exposure is shown by Figure 27.

The decrease of capacity was initially attributed to a loss of amine impregnate from the charcoal. During the study, however, the effluent of both absorption and regeneration flow was monitored for ammonia vapor and subsequent analysis indicated a piperazine loss of only 232 mg or 2.2% of the initial loading. The degradation of CO_2 capacity could not be attributed to piperazine loss alone.

The effect of process flowrate or residence time on this sorber was then evaluated. The process flowrate was decreased from 5 to 1 lpm thereby increasing the residence time from 1 to 5 seconds. The breakpoint and saturation sorber CO_2 concentration for cycles 22 through 24 were 0.010 and 0.015 lb CO_2/lb sorber, respectively. These values were compared to 0.010 and 0.019 lb CO_2/lb sorber for 5 lpm flowrate used with cycle 21.

CO_2 partial pressures of 1, 3.7 and 5.9 mm Hg were studied with a 5 lpm flowrate in cycles 25 through 30. In cycles 25 and 26, 1 mm Hg CO_2 partial pressure, the mean breakpoint and saturation concentrations were 0.0058 and 0.0064 lb CO_2/lb sorber, respectively. Cycles 27 and 28, 5.9 mm Hg CO_2 partial pressure, yielded 0.0040 and 0.0078 lb CO_2/lb sorber for the breakpoint and saturation concentration. The CO_2 partial pressure for cycles 29 through 31 was 3.7 mm Hg for which the associated concentrations were 0.0055 and 0.011 lb CO_2/lb sorber. Although the data indicate that the saturation concentration is greatest for 3.7 mm Hg, the quantities of sorber and measured CO_2 capacity should be considered similar for the range of CO_2 partial pressure studied.

During cycles 32 through 42, the effect of sorber moisture content on CO_2 capacity was studied. The observed capacities for moisture contents in the range of 5 to 24 wt % were 0.004 to 0.007 lb CO_2/lb sorber similar to the capacities determined during the CO_2 partial pressure experiments.

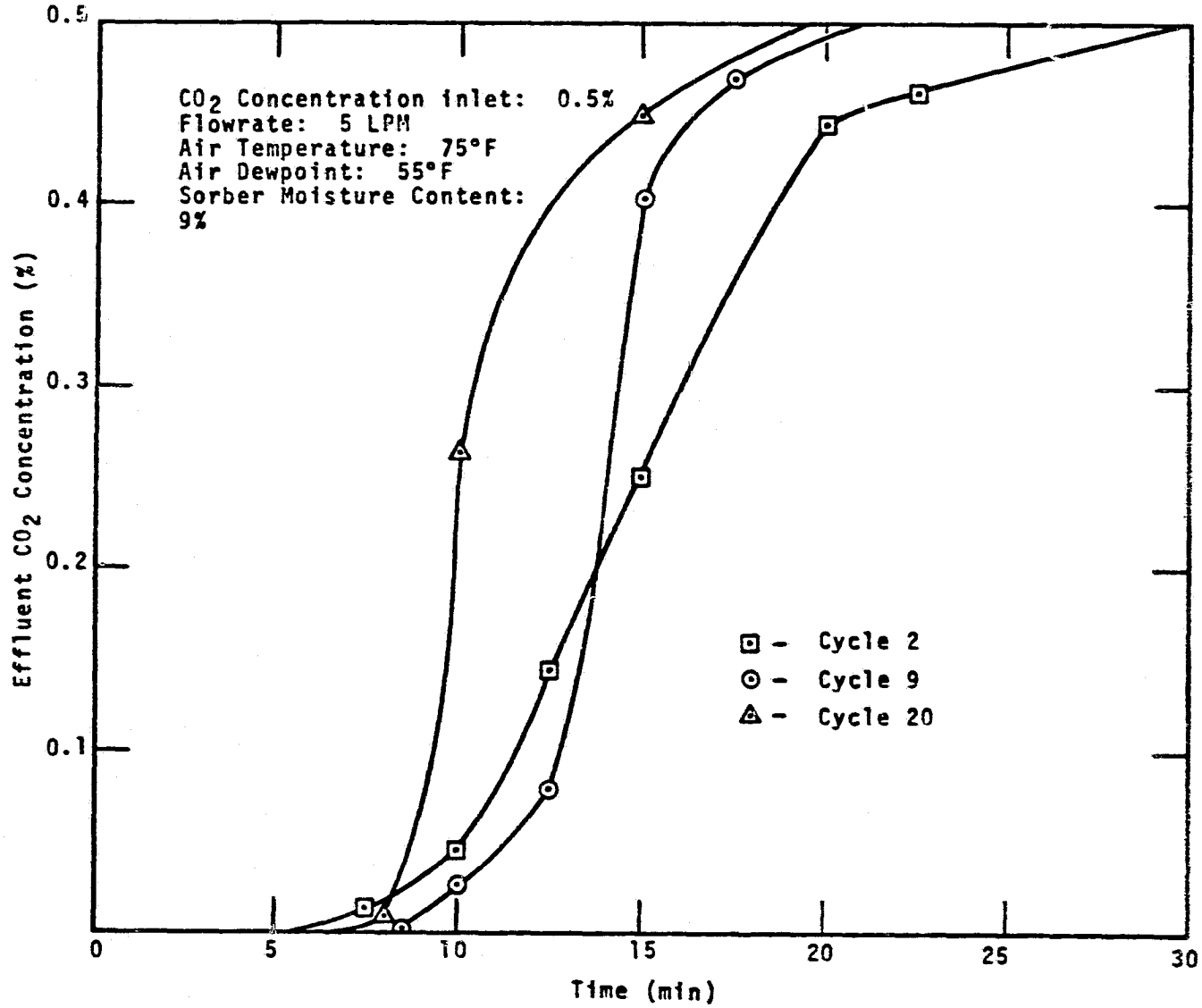

FIGURE 26 BREAKTHROUGH CURVES FOR CARBON-AMINE

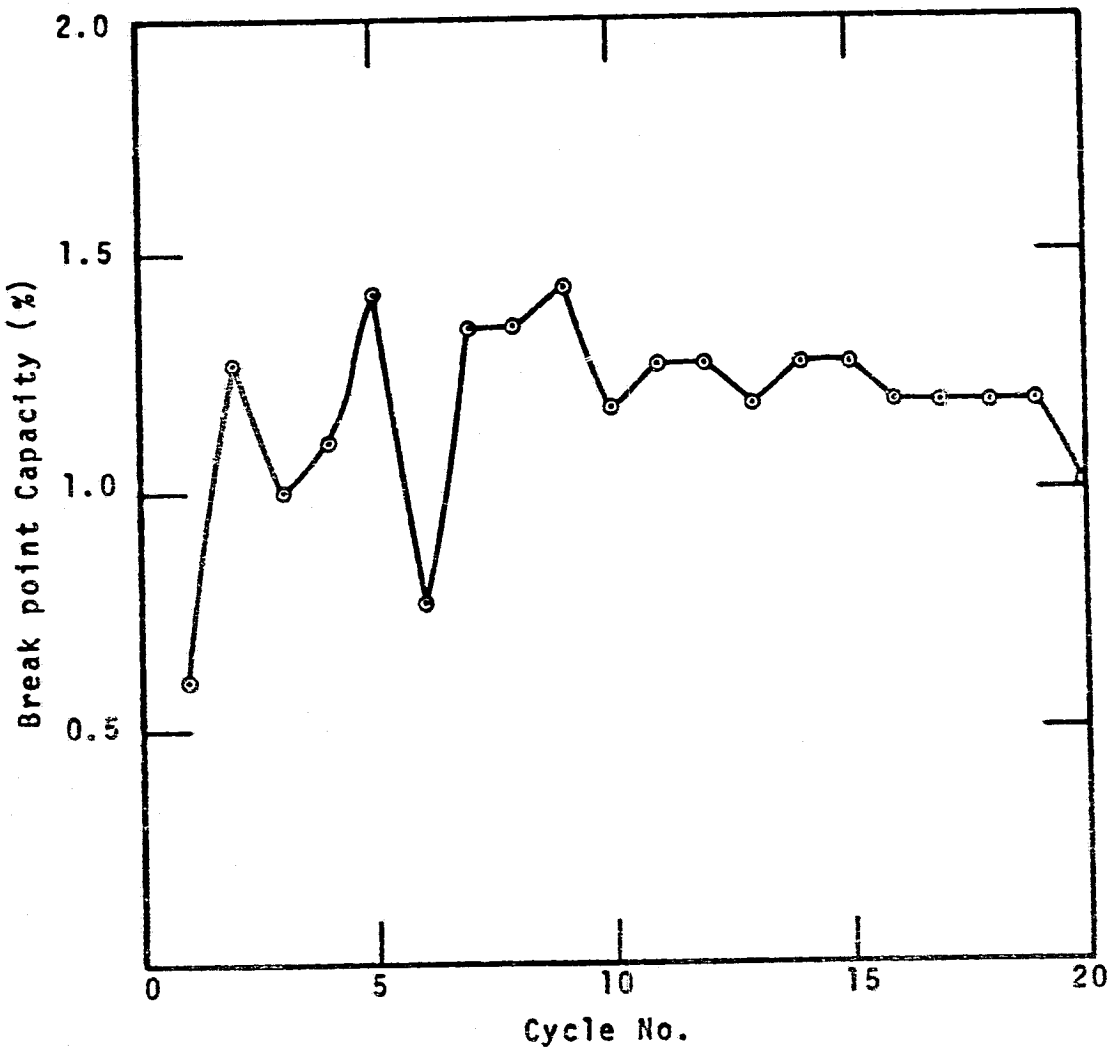

CYCLING EFFECT ON CARBON-AMINE BREAK CAPACITY

FIGURE 27

TASK V 90-DAY TEST SUPPORT

Included in this task were performance testing a sorber bed supplied by Hamilton-Standard Division of United Aircraft Corporation and analysis of data obtained under Contract No. NAS1-5277 and NAS1-7263 in support of the polymeric type CO_2 concentration system used in the NASA-LRC 90-day manned test performed by McDonnell Douglas Astronautics Company - Western Division.

The sorber bed was MOL prototype hardware which was designed for a zeolite type CO_2 sorber. Data obtained in Task I of Contract No. NAS1-7263 indicated that the MOL sorber bed could be used in an IR-45, steam regenerable CO_2 concentration system. Three MOL sorber beds were made available and one was delivered to MSA for testing in a 4-man size system. The bed was 6 in. ID x 11 in. long and a 4-way disk valve, pneumatically operated, located at one end of the bed controlled the process air inlet, outlet, steam inlet and CO_2 outlet. The bed was filled with 6.7-8.0 lb IR-45 with 15% moisture content and subjected to continuous absorption-regeneration cycles with the following process conditions:

1. CO_2 input rate: 0.4 lb/hr
2. CO_2 input partial pressure: 3.7 mm Hg
3. Total pressure: 7 and 14.3 psia
4. Process air flowrate: 5-19 ACFM
5. Process air temperature: 75-90°F
6. Process air dewpoint: 40-70°F
7. Steam flowrate: 1.7-3.2 lb/hr

Initially it was thought a 3-bed system with two beds operating in parallel and each containing 7 lb IR-45 would be required to remove 0.4 lb CO_2/hr from a cabin atmosphere containing 4 mm partial pressure CO_2. This capability would require that the mean CO_2 capacity of each bed be 0.019 lb CO_2/lb IR-45. For a total pressure of 7 psia, the process flowrate required to input 0.4 lb CO_2/hr at 80°F, is 12.2 ACFM considering the 100% CO_2 removal efficiency.

Performance data obtained during the tests included sorption efficiency, CO_2 capacity, steam required for regeneration, desorbed gas flowrate and CO_2 purity.

Also, several samples of IR-45 were evaluated for flammability, odor and off-gas characteristics by the NASA Manned Spacecraft Center prior to being included in the 90-day test. Procedures for these evaluations are described by reference 4.

Results

Seven test series were performed with the MOL sorber bed. Test series I, II, IV and V were performed at 7 psia while for series III the total pressure was 14.3 psia.

Series I, II, III and IV were performed with 75-80°F process air temperatures, 55-67°F process air dewpoints, 30 minute absorption time, 1.7 lb/hr of 220-225°F steam and 12-19 ACFM process air flowrates. The sorber bed contained 7.0 ± .25 lb IR-45 with a 15% moisture content. CO_2 capacities of 0.021-0.023 lb CO_2/lb IR-45 were observed during these tests but the IR-45 became moisture laden after 3-5 cycles of operation. The increase of IR-45 moisture content was indicated both by the reduction of CO_2 removal and increasing regeneration time. The first and second regeneration of a test series were performed in 23-25 minutes with a regeneration pressure of 11-12 psia using a steam rate of 1.7 lb/hr equivalent to 0.131 lb steam/lb dry IR-45. The regeneration time then increased to 33-35 minutes and 0.184 lb steam/lb dry IR-45 as the IR-45 moisture content increased.

Test series V was also performed at 7 psia total pressure but the process air dewpoint was 45 ± 2°F; the process air temperature was 82 ± 2°F and the process flowrate 13 ACFM. The absorption time was 40 minutes with 1.7 lb/hr steam rate and 11-12 psia regeneration pressure. These conditions were operated for eight cycles with the IR-45 moisture content maintained at 21-23% at the end of absorption. During the 40 minute absorption, 0.15 lb CO_2 was absorbed by 7.2 lb IR-45 for a capacity of 0.021 lb CO_2/lb IR-45. Regeneration was performed in 28-31 minutes requiring 0.148 lb steam/lb dry IR-45.

Series VI tests were performed similarly to series V except that 8.0 lb IR-45 with a 15% moisture content was placed into the sorber bed and the steam rate was increased to 3.2 lb/hr. Operation was maintained for 9 cycles with the IR-45 moisture content maintained at 21-24% for 7 cycles. An increase of system pressure drop was observed during the ninth cycle and the test terminated. The sorber bed was then opened and the IR-45 was found to have expanded and was packed tightly against the outlet screen. Although 0.15 lb CO_2 with a maximum of 0.19 lb CO_2 was absorbed during the successful 40 minute absorptions, the bed could not accommodate the expansion of the IR-45. Regeneration was performed in 17-20 minutes reflecting a steam requirement of 0.142-0.167 lb steam/lb dry

IR-45. During the regeneration of series VI tests, 0.066-0.092 lb of water were condensed from the CO_2-steam separation when the steam front broke through the bed.

For the series VII tests, 7.3 lb IR-45 were placed into the sorber bed for the concluding test of the MOL sorber bed. The bed was successfully operated through 14 cycles with 76-86°F air temperature, 40-43°F dewpoint and 10-16 ACFM process flowrate. The air temperature and/or process flowrate were controlled for an individual absorption to determine if immediate degeneration of CO_2 removal and IR-45 moisture content would occur. The sorber achieved an apparent steady state CO_2 removal capacity of 0.018 lb CO_2/lb IR-45 for tests with 15-16 ACFM process flowrate and 40 minute absorption. Regeneration was performed with 1.7 lb/hr steam rate in 23-27 minutes for a steam requirement of 0.112-0.132 lb steam/lb dry IR-45. Figures 28 and 29 present the cumulative regeneration evolved gas volume and evolved gas flowrate with regeneration time. Noted on the data are the evolved gas temperature and point at which the CO_2-air separation occurred and the oxygen concentration of the evolved gas became less than 0.2%. The CO_2 steam separation occurred with 0.026-0.064 lb water condensed from the steam front. Table 13 presents the absorption-regeneration results of the series VII tests.

TABLE 13 - SERIES VII TEST RESULTS

Test No.	Reg. Time (min)	Flowrate (ACFM)	CO_2 Abs. (lb)	Steam Condensed (lb)
VII a	40/17	14	0.126	0.064
b	40/17	9	0.120	0.070
c	40/19	14	0.128	0.062
d	40/22	12	0.080	0.055
e	40/23	14	0.147	0.035
f	40/24	16	0.133	0.035
g	40/27	15	0.134	0.026
h	40/26	15	0.147	0.048
i	40/27	14	0.107	0.053
j	40/25	11	0.078	0.055
k	40/25	16	0.064	0.051
l	40/26	16	0.101	0.058
m	40/2[illegible]	18	0.127	0.055

The results of these tests were forwarded to Hamilton-Standard with the recommendations that:

1. Three bed system would remove 0.4 lb/hr at 4 mm Hg CO_2 partial pressure and 16 ACFM process flowrate.

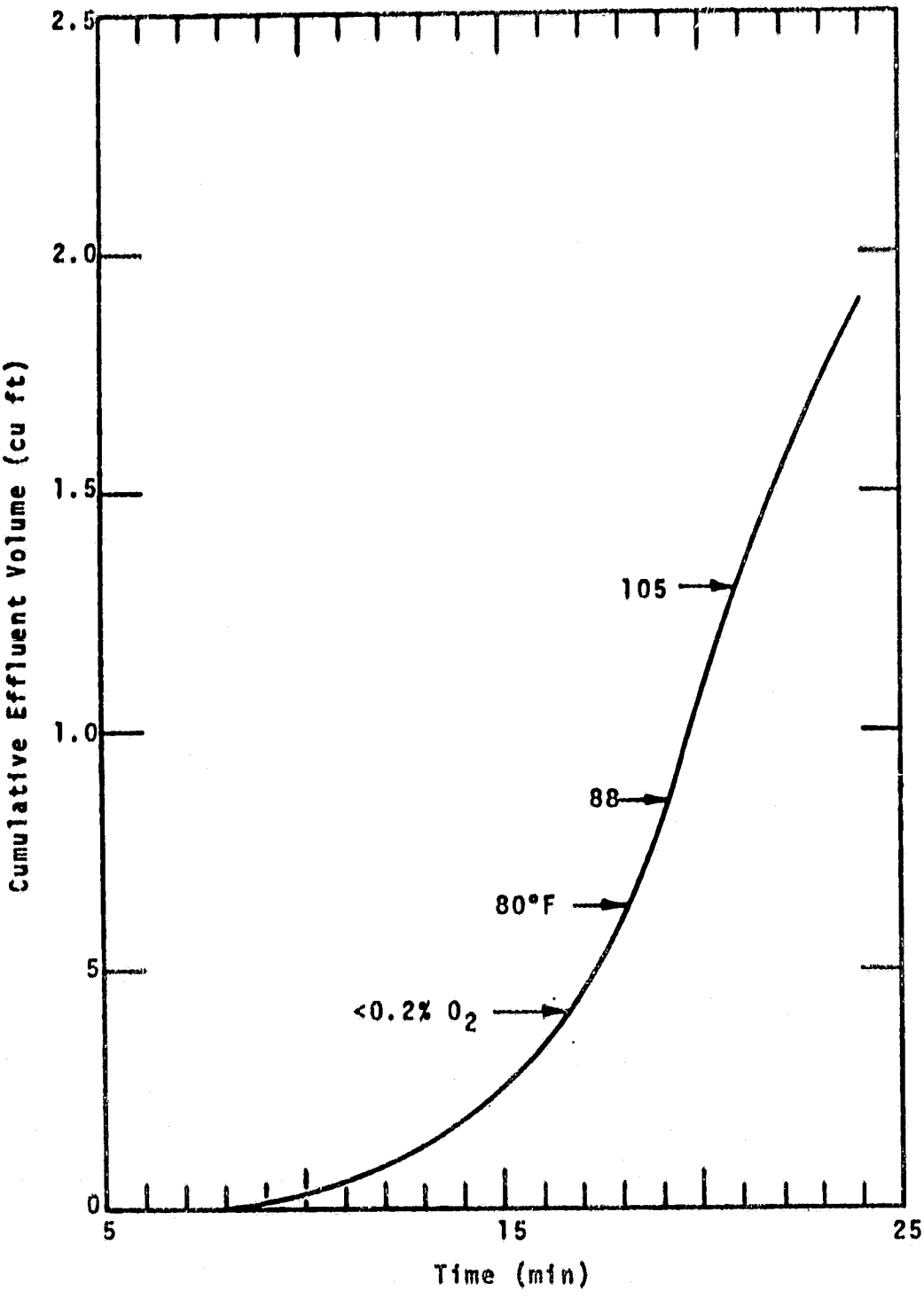

FIGURE 28 CUMULATIVE REGENERATION VOLUME HISTORY

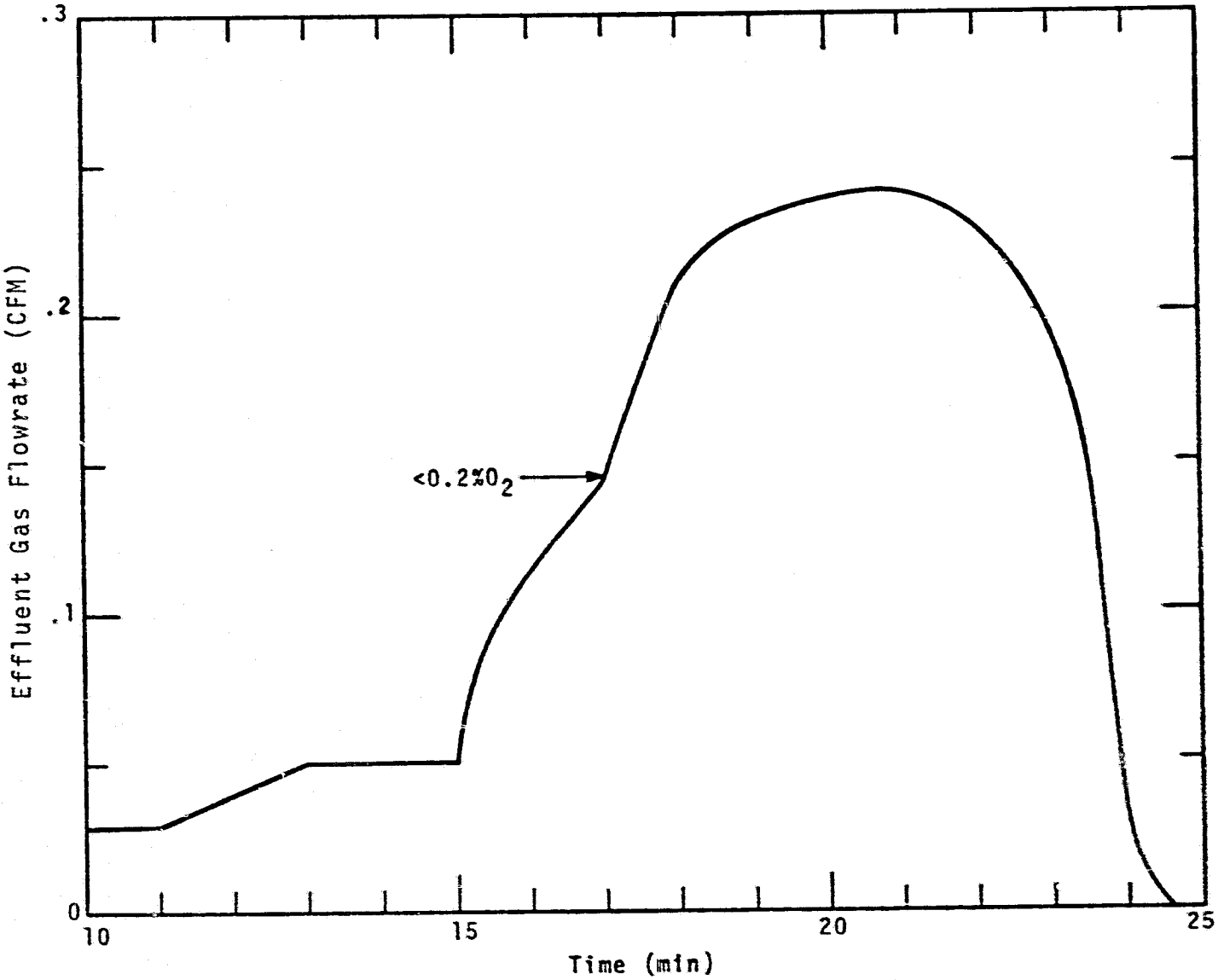

FIGURE 29 REGENERATION OF MOL BED

2. CO_2-air separation could be detected by increase of evolving gas flowrate and this mode of control should be used rather than time.

3. 0.06 lb steam would break through sorber bed at the conclusion of regeneration which would be indicated by steam temperature.

4. Concentrated CO_2 purity of 98% could be expected.

Evaluation of the flammability, odor and off-gas characteristics were performed on samples of "as received", steam cycled, methanol washed and methanol extracted plus steam exposed IR-45. The "as received" IR-45 used for these evaluations had not been exposed to CO_2 absorption and regeneration tests. The IR-45 received from the manufacturer was dried and then moisture added to increase the moisture content to 20%. The steam cycled IR-45 sample was taken from material which had been exposed to CO_2 absorption and regeneration for 30 cycles which totalled approximately 12 hours of steam exposure.

The sample of methanol washed IR-45 was taken from material which had been submerged in 140°F methanol for 4-6 hours, rinsed with distilled water and vacuum dried. The methanol extracted plus steam exposed sample was taken from IR-45 which had been exposed to Soxhet extraction, using methanol as described in Task I, then exposed to continuous steam for 8 hours and vacuum dried.

Flame propagation tests were conducted in a 100 mm O_2/260 mm N_2 environment. Each of the samples yielded a 0.0 in./sec propagation rate. Flash and fire point tests were conducted in 100 mm O_2/260 mm N_2 and 320 mm O_2 environments to a temperature of 599°F. Each sample charred at 356°F indicating thermal decomposition but no flash or fire points were observed. A "pass" rating was given for IR-45 flammability.

The odor evaluation was performed by a ten member panel which rated the odor according to the following scale:

Panel Member Rating	Numerical Rating
Undetectable	0
Barely detectable	1
Easily detectable	2
Objectionable	3
Irritating	4

A maximum of 2.5 is permitted for a "pass" rating.

For each odor evaluation, 5.0 ± 0.1 grams/liter, at ambient pressure, was the weight of IR-45 to test chamber volume fraction. Each of the samples was evaluated by the panel at concentrations of 1/29 parts O_2, 1/9 parts O_2 and no dilution. The predominant odor noted by the evaluation was ammonia-like and an ammonia concentration of <10 μ grams/gram IR-45 was observed. Table 14 presents the odor evaluation results.

The off-gas evaluation considered CO and total organics. A concentration of 25 μ grams/gram and 100 μ grams/gram were required for a "pass" rating for CO and total organics, respectively. The results of the off-gas evaluation of IR-45 are presented by Table 15.

TABLE 14 - ODOR EVALUATION RESULTS

Sample	Odor Sample Concentration	Numerical Rating
"as received"	1/29 parts O_2	1.2
	1/9 parts O_2	2.2
	no dilution	3.5
steam cycled	1/29 parts O_2	0.5
	1/9 parts O_2	1.0
	no dilution	3.2
methanol washed	1/29 parts O_2	1.5
	1/9 parts O_2	2.7
	no dilution	3.6
methanol extracted plus steam exposed	1/29 parts O_2	2.0
	1/9 parts O_2	2.1
	no dilution	3.5

TABLE 15 - RESULTS OF IR-45 OFF-GAS EVALUATION

Sample	Total Organics	Carbon monoxide
"as received"	12 μ g/g	25 μ g/g
methanol washed	0.7 μ g/g	114 μ g/g
steam cycled	1.4 μ g/g	15 μ g/g
methanol extracted plus steam exposed	2.2 μ g/g	42 μ g/g

CONCLUSIONS AND RECOMMENDATIONS

Studies with IR-45 as a CO_2 sorber and concentrator have shown:

1. IR-45 particle size does not strongly affect CO_2 sorption but is significant for minimizing sorber pressure drop. Particles greater than 30 mesh permit a 100% pressure drop reduction compared to the "as received" 16-60 mesh material.

2. Process air flowrate and sorber bed geometry can be combined into a residence time parameter to measure CO_2 sorption efficiency. Absorption efficiency decreases from 0.86 to 0.75 as the residence time decreased from 1.5 to 0.7 sec. The cyclic CO_2 absorption decreased from about 2% to 1% for the same residence time range.

3. The CO_2 absorption wave speed through an IR-45 bed increases linearly with process flowrate. Increasing the process flowrate from 100 to 260 lb/hr ft^2 resulted in a wave speed increase from 0.5 to 1.8 in./min.

4. Toluene was identified as the primary contaminant offgassed from the IR-45 during the absorption cycle following steam regeneration. Methanol pretreatment of IR-45, prior to use, reduced the toluene concentration from 10,000 to 200 μ gm/m^3.

   An off-gas, flammability and odor evaluation performed by NASA-MSC rated IR-45 "passing" for total organics, carbon monoxide, flammability and odor.

5. The change from 100% air to 99% CO_2 occurs within 1 minute independent of IR-45 particle size or bed geometry. The gas flowrate increases dependent upon steam flowrate and quantity of CO_2 and this flowrate increase may be used as a control point for switching from air displacement to CO_2 concentration. CO_2 may be concentrated at 98% purity with 97% recovery.

6. The saturation capacity of IR-45 is non-linearly and directly related to CO_2 partial pressure in the 0.8 to 15 mm Hg range. For 1 and 3.7 mm Hg CO_2 partial pressure, the saturation capacity is 2 and 2.7%. Thus, IR-45 demonstrates a more favorable isotherm than molecular sieve at 1 mm Hg p_{CO_2} control level.

7. The absorption of CO_2 by IR-45 is apparently independent of total pressure in the 7 to 15 psia range.

8. A three-bed system offers a 24-32% reduction of unit weight CO_2 concentration energy over a one-bed system.

9. Maintaining the IR-45 moisture content throughout the bed between 12 and 25% is the primary factor influencing the CO_2 concentration process.

10. The process model which limits the air to saturation but includes a recondensation effect (fog) shows the most merit for predicting the operational behavior of the IR-45 CO_2 concentration process.

11. A piprazine impregnated charcoal type CO_2 sorber exhibited a lesser dependence, than IR-45, of CO_2 sorption characteristics on moisture content. However, absorption capacity decreased over as few as 20 cycles.

Primary recommendations include:

1. Refinement of process model to improve correlation with experimental results.

2. Advance CO_2 sorber to obtain material with lower heat capacity, broader operational moisture content range, greater CO_2 capacity at 1 mm Hg CO_2 partial pressure and greater mass transfer rate.

```
C PROGRAM ENWD
 DIMENSION W(33),TB(33)
 ACCEPT 2,W1,W2,W3
 ACCEPT 2,H1,AK1,DO,PWST
 ACCEPT 2, CPA,CPS,CPW,CPB
2 FORMAT (E)
 ACCEPT 2, R,V1, P
 ACCEPT 2, WWB
 ACCEPT 2, AL,AREA
       V1=V1/AREA
 TYPE 3
3 FORMAT (/,"TEMP BED",/)
 ACCEPT 2, TIP
 ACCEPT 2,01,TBL,TBH,TEX,T1
 DO 4 I=1,33
 TB(I)=TIP
 W(I)=WWB
4 CONTINUE
6 TYPE 7
7 FORMAT ( /,"HEAT       MASS TRANS",/)
 SUM=0.0
 DL=AL/32.0
 O=0.0
C
C POINT A2
C
 DO 13 I=1,30
 DO 15 IJ=1,50
 T22=T1
 VJ=V1
 PAJ=PWST
C
C POINT A3
C
 DO 14 J=1,32
 T2=TB(J)+460.0
 ISW=1
 GO TO 1000
1001 H=H1*(VJ)
 AK=AK1*(VJ)
C
C POINT A4
C
 IF (W(J)-0.277) 16,16,17
16 PRW=PRW*(0.6322+1.3278*W(J))
17 DELW= AK*18.0*LOGF((P-PRW)/(P-PAJ))
20 DELQ=H*(T22-TB(J))
 DELT=DELQ+DELW*CLA
 DELT=DELT/(CPB+CPW*W(J))
 DELT=DELT/R*DO
 TBX=TB(J)+DELT

*
```

```
22 TB(J)=TBX
 W(J)=W(J)+DELW/R*DO
 VJ1=VJ-DELW/18.0*DL
 PAV=-DL*DELW/18.0*P+PAJ*VJ
 PAJ1=PAV/VJ1
 PAV=DELQ+DELW/18.0*TB(J)*CPS
 PAV=-PAV*DL+T22*VJ*(CPA+PAJ/P*(CPS-CPA))
 T22=PAV/VJ1/(CPA+PAJ1/P*(CPS-CPA))
31 T2=T22+460.0
 ISW=2
 GO TO 1000
1002 IF (PRW-PAJ1) 30,32,32
30 DELW=PAJ1*0.05/P
 IF (DELW-0.001) 33,33,34
 34 DELW=0.001
33 CLA=CLA*DELW*18.0
 TBX=VJ1
 VJ1=(1.0-DELW)*TBX
 PAJ1=PAJ1-DELW*P
 DELW=TBX*DELW*DO*18.0/R/DL
 W(J)=W(J)+DELW
 DELQ=CPW*(T22-TB(J))*DELW
 T22=T22+CLA*TBX/VJ1/(CPA+PAJ1/P*(CPS-CPA))
 TB(J)=TB(J)+DELQ/(CPB+W(J)*CPW)
 GO TO 31
32 PAJ=PAJ1
 VJ=VJ1
14 CONTINUE
C
C POINT A5 ──────────────────┐
C                            ▼
 O=O+DO
 IF (O-O1) 15,25,25
25 X1=TBL-TB(7)
 X2=TBH-TB(25)
 X3=TEX-T22
 SUM=SUM+W1*X1*X1+W2*X2*X2+W3*X3*X3
 TYPE 27, TBL,TB(7),TBH,TB(25),TEX,T22
27 FORMAT (/,E,E)
 ACCEPT 2, O1,TBL,TBH,TEX,T1
 IF (O1)          28,28,15
15 CONTINUE
13 CONTINUE
28 TYPE 26,SUM
26 FORMAT (/,"SUM SQS",E)
 STOP
1000 CLA=1094.78-0.58242*(T2-460.0)
 PRW=48.6956 -11873.6/T2-4.353*LOGF(T2)
 PRW=EXPF(PRW)
 GO TO (1001,1002),ISW
 END

*
```

LIST OF SYMBOLS

A_p	Specific packing surface	sq ft/cu ft
C_p	Heat capacity	BTU/mole-°F
C_{pa}	Heat capacity of air	BTU/mole-°F
C_{pb}	Heat capacity of IR-45	BTU/lb-°F
C_{ps}	Heat capacity of steam	BTU/mole-°F
C_{pw}	Heat capacity of water	BTU/lb-°F
G	Mass flowrate	moles/hr-sq ft
G'	Mass flowrate	lb/hr-sq ft
K	Mass transfer coefficient	moles/min-cu ft
L	Mass flowrate (liquid)	moles/hr-sq ft
L'	Mass flowrate (liquid)	lb/hr-sq ft
P	Pressure	psi
ΔP	Pressure drop	psi
p_{aw}	Water vapor partial pressure	psi
p_{rw}	Water vapor saturation pressure	psi
Q	Heat	BTU
del Q	Heat flowrate	BTU/min-cu ft
Re	Reynolds number	
T	Temperature	°F
ΔT	Temperature difference	°F
V	Molar flowrate	moles/min-sq ft
W	IR-45 moisture content	lb/lb
del W	Mass flowrate	lb/min-cu ft
X*	Saturation capacity	percent
Z	Bed depth	ft

LIST OF SYMBOLS (continued)

a, b	Constants	
dp	$6(1-\varepsilon)/Ap$	ft
g'c	4.18×10^8	lb ft/$lb_f hr^2$
h	Heat transfer coefficient	BTU/min-cu ft
m, n	Shape factor	
ε	Bed void fraction	
p	Density	lb/cu ft
θ	Time	minutes
λ	Latent heat of vaporization	BTU/lb
μ	Viscosity	lb/ft sec

REFERENCES

1. Mass Transfer Operations, Treybal, R.E., 2nd Edition, 1968, McGraw-Hill Book Company, New York.

2. Mass Transfer Operations, Treybal, R.E., 1955, McGraw-Hill Book Company, New York.

3. Vancheri, F., MSA Research Corporation.

4. Procedures and Requirements for the Flammability and Off-gassing Evaluation of Manned Spacecraft Nonmetallic Materials, NASA Document D-NA-0002.